Middle to late Cenozoic basin evolution in the western Alborz Mountains: Implications for the onset of collisional deformation in northern Iran

Bernard Guest,[1,2] Brian K. Horton,[1,3] Gary J. Axen,[1,4] Jamshid Hassanzadeh,[5] and William C. McIntosh[6]

Received 4 December 2006; revised 7 May 2007; accepted 19 July 2007; published 21 December 2007.

[1] Oligocene-Miocene strata preserved in synclinal outcrop belts of the western Alborz Mountains record the onset of Arabia-Eurasia collision-related deformation in northern Iran. Two stratigraphic intervals, informally named the Gand Ab and Narijan units, represent a former basin system that existed in the Alborz. The Gand Ab unit is composed of marine lagoonal mudstones, fluvial and alluvial-fan clastic rocks, fossiliferous Rupelian to Burdigalian marine carbonates, and basalt flows yielding $^{40}Ar/^{39}Ar$ ages of 32.7 ± 0.3 and 32.9 ± 0.2 Ma. The Gand Ab unit is correlated with the Oligocene–lower Miocene Qom Formation of central Iran and is considered a product of thermal subsidence following Eocene extension. The Narijan unit unconformably overlies the Gand Ab unit and is composed of fluvial-lacustrine and alluvial fan sediments exhibiting contractional growth strata. We correlate the Narijan unit with the middle to upper Miocene Upper Red Formation of central Iran on the basis of lithofacies similarities, stratigraphic position, and an 8.74 ± 0.15 Ma microdiorite dike ($^{40}Ar/^{39}Ar$) that intruded the basal strata. Deformation timing is constrained by crosscutting relationships and independent thermochronological data. The Parachan thrust system along the eastern edge of the ancestral Taleghan-Alamut basin is cut by dikes dated at 8.74 ± 0.15 Ma to 6.68 ± 0.07 Ma ($^{40}Ar/^{39}Ar$). Subhorizontal gravels that unconformably overlie tightly folded and faulted Narijan strata are capped by 2.86 ± 0.83 Ma ($^{40}Ar/^{39}Ar$) andesitic lava flows. These relationships suggest that Alborz deformation had migrated southward into the Taleghan-Alamut basin by late Miocene time and shifted to its present location along the active range front by late Pliocene time. Data presented here demonstrate that shortening in the western Alborz Mountains had started by late middle Miocene time. This estimate is consistent with recent thermochronological results that place the onset of rapid exhumation in the western Alborz at ~12 Ma. Moreover, nearly synchronous Miocene contraction in the Alborz, Zagros Mountains, Turkish-Iranian plateau, and Anatolia suggests that the Arabia-Eurasia collision affected a large region simultaneously, without a systematic outward progression of mountain building away from the collision zone. **Citation:** Guest, B., B. K. Horton, G. J. Axen, J. Hassanzadeh, and W. C. McIntosh (2007), Middle to late Cenozoic basin evolution in the western Alborz Mountains: Implications for the onset of collisional deformation in northern Iran, *Tectonics*, *26*, TC6011, doi:10.1029/2006TC002091.

1. Introduction

[2] Iran is a key region for studying collisional processes and plateau development because the recent Arabia-Eurasia collision provides insight into the early histories of mature collisional orogens such as the Indo-Asian and Alpine collision zones and orogenic plateaus such as the Tibetan and Altiplano plateaus. Crustal shortening in the Alborz Mountains of northern Iran (Figure 1), a 2- to 5-km-high range defining the boundary between the Turkish-Iranian plateau and the Caspian basin, is kinematically linked to the Arabia-Eurasia collision to the south [*Stöcklin*, 1968, 1974; *Berberian and King*, 1981; *Berberian*, 1983; *Sengor*, 1990; *Alavi*, 1996; *Axen et al.*, 2001; *Allen et al.*, 2003, 2004; *Guest et al.*, 2006a]. This relationship makes the timing and magnitude of Cenozoic deformation in the Alborz important for constraining the overall spatiotemporal evolution of the collision zone.

[3] Despite the youthfulness of the collision, the timing of initial shortening and associated basin formation in the Alborz Mountains remains uncertain. Apatite and zircon (U-Th)/He and K-feldspar $^{40}Ar/^{39}Ar$ thermochronological data from four plutons in the western Alborz are interpreted as indicating an onset of rapid exhumation between ~12 Ma and 5 ± 2 Ma [*Axen et al.*, 2001; *Guest et al.*, 2006b].

[1]Department of Earth and Space Sciences, University of California, Los Angeles, USA.
[2]Now at Geology Section, Department of Geological and Environmental Sciences, Ludwig-Maximilians-University, Munich, Germany.
[3]Now at Institute for Geophysics and Department of Geological Sciences, Jackson School of Geosciences, University of Texas, Austin, Texas, USA.
[4]Now at Department of Earth and Environmental Science, New Mexico Institute of Mining and Technology, Socorro, New Mexico, USA.
[5]Department of Geology, University of Tehran, Tehran, Iran.
[6]New Mexico Geochronology Research Laboratory, New Mexico Institute of Mining and Technology, Socorro, New Mexico, USA.

0278-7407/07/2006TC002091$12.00

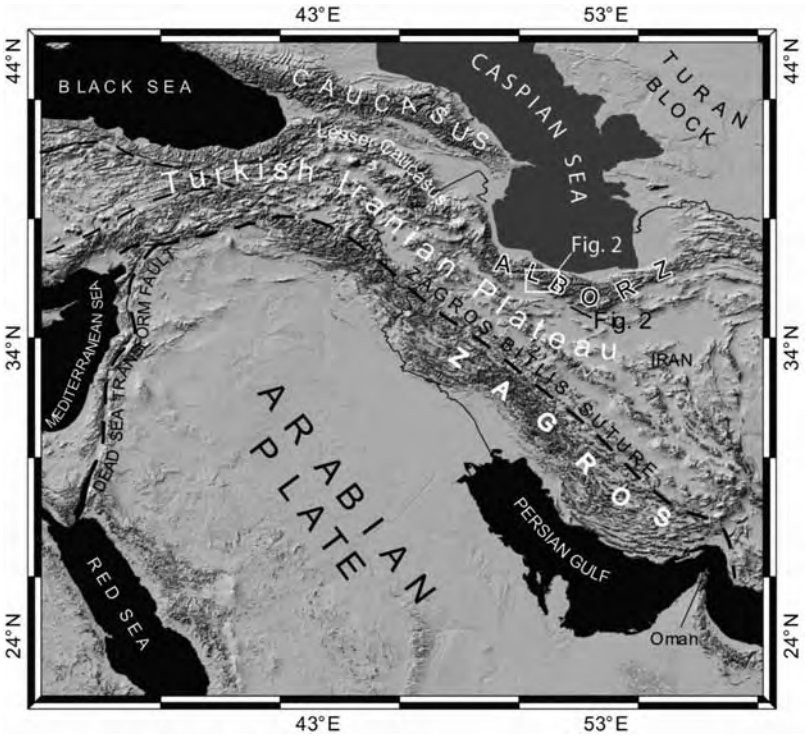

Figure 1. Shaded relief map showing the Arabia-Eurasia collision zone. Iran's border is shown in black. Labels refer to major physiographic and tectonic units. The box over the western Alborz Mountains shows the location and coverage of Figure 2.

However, on the basis of limited preservation of Oligocene strata, *Allen et al.* [2003] suggest that contractional deformation in the Alborz began as early as Oligocene time and continued to the present. Similarly, *Vincent et al.* [2005] speculate that slope instability features in the Talesh Mountains farther west record the onset of shortening-induced uplift and exhumation in northern Iran during late Eocene–early Oligocene time.

[4] In this paper we examine stratigraphic, sedimentologic, and geochronological evidence for Neogene collisional deformation preserved in two synformal basins of the western Alborz. The aim is to provide constraints on the timing of initial shortening in northern Iran that are independent of previous thermochronological constraints [e.g., *Axen et al.*, 2001; *Guest*, 2004; *Guest et al.*, 2006b] and provide a more direct linkage between deformation and sedimentation than previous interpretations [e.g., *Allen et al.*, 2003]. We focus on Oligocene-Miocene strata of the Taleghan basin and to a lesser extent on correlative strata of the Alamut basin (Figure 2). In contrast to previous interpretations of two independent intermontane basins [e.g., *Annells et al.*, 1975a, 1975b; *Davoudzadeh et al.*, 1997], we identify a depositional link between the two outcrop belts and suggest they represent remnants of a single, larger ancestral Taleghan-Alamut basin. In addition, we examine an unconformity within the lower Taleghan succession to determine whether rocks above and below the unconformity were deposited in different tectonic regimes (e.g., collisional versus precollisional) and to estimate the amount of time the unconformity represents. We also present new age constraints obtained from a marine fossil assemblage and $^{40}Ar/^{39}Ar$ whole rock and hornblende analyses of lava flows and dikes. Finally, we discuss our observations and interpretations in the context of precollisional and collisional deformation in northern Iran and highlight their significance in understanding the development of the Arabia-Eurasia collision zone.

2. Structural Geology

[5] To better understand the structural and stratigraphic evolution of the Cenozoic basin system described here, an explanation of the regional stratigraphy of the Alborz Mountains is provided (available as auxiliary material; including Figure S1[1]). Oligocene-Miocene rocks of the Taleghan and Alamut basins (Figure 2) occur within two E trending synclines associated with a series of E and SE striking thrust systems in the western Alborz (Figure 2). These thrust systems involve Neoproterozoic-Phanerozoic rocks, exhibit variable dips and vergence directions, and display kinematic indicators suggesting dextral transpression [*Guest et al.*, 2006a]. A broad, E plunging anticline consisting of Eocene Karaj Formation volcanic rocks composes the Kuh-e-Alborz range (Figure 3), which separates exposures of the Alamut basin to the N from the Taleghan basin to the S (Figure 2). The S margin of the Taleghan basin is bounded by two thrust systems: the SE striking

[1]Auxiliary material data sets are available at ftp://ftp.agu.org/apend/tc/2006tc002091. Other auxiliary material files are in the HTML.

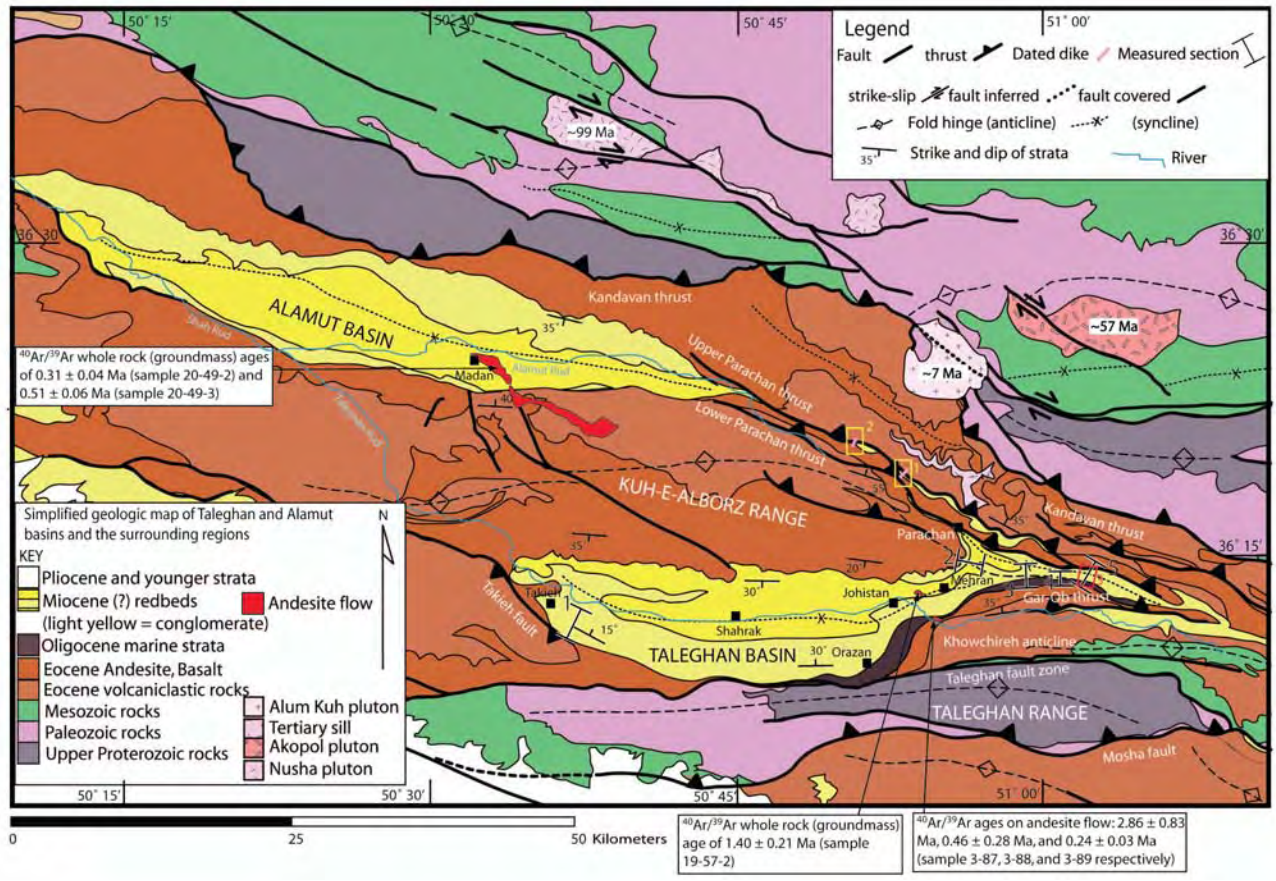

Figure 2. Simplified geologic map showing regional geology of the western Alborz in relationship to the Taleghan and Alamut basins. Ages for the dated andesite flows are shown. Yellow boxes with numbers indicate dated dikes. Red box indicates the location of the Gand Ab basalt. Box 1, sample 19-137-1: 8.74 ± 0.15 Ma; Box 2, samples 84-2b, 4-84-2a, and 4-86-3 give ages of 7.31 ± 0.10 Ma, 7.06 ± 0.08 Ma, and 6.68 ± 0.07 Ma respectively; Box 3 (red), sample 19-135-1, and 19-133-1 give ages of 32.8 ± 0.2 Ma and 32.7 ± 0.3 Ma respectively (Tables 1 and 2).

Takieh fault at the W end of the basin, and the E striking Taleghan fault zone which bounds the Taleghan range to the S and joins the sinistral reverse Mosha fault farther east (Figure 2). The E limits of both the Taleghan and Alamut basins are defined by SE striking thrusts of the Parachan fault zone which merge southeastward with the E striking Gar Ob thrust that parallels the Khowchireh anticline. Finally, in the N parts of the study area, the Kandavan thrust approximates the N limit of the Alamut basin (Figure 2).

[6] The Taleghan basin is 50 km long, up to 12 km wide, and passes eastward from a structurally simple syncline to faulted and folded basin remnants (Figure 2). Most post-Eocene sediment is preserved in the core of the large, E trending, doubly plunging Taleghan syncline bounded by the Kuh-e-Alborz anticline to the N and several fault systems along its other margins (Figure 2). Strata within this syncline are folded into a series of localized upright anticlines and synclines with hingelines trending subparallel to the basin margins. Internal deformation in the basin increases laterally with folds becoming tighter and more numerous from W to E (Figure 2).

[7] In W Taleghan basin, the Takieh fault (Figure 2) dips 60° SW, places Eocene Karaj Formation over basin fill, and has striae and mineral fibers that indicate oblique, reverse-sinistral slip. In the hanging wall, Karaj volcanic flows are folded into an anticline and cut by the fault in a hanging wall ramp cutoff relationship (Figure 4a). The footwall is composed of vertical to overturned conglomeratic growth strata of the Miocene Narijan unit that form the S limb of a growth syncline. The growth strata thicken northward across the hinge of the syncline and display near-horizontal dips in the N limb (Figures 4b and 5a). The Takieh fault terminates or is covered along strike to the SE where basin fill rests directly on Karaj lavas (Figure 2).

[8] The E striking Taleghan fault zone (Figure 2) juxtaposes Neoproterozoic-Mesozoic rocks of the Taleghan range to the S against rocks of the Taleghan basin. Along most of the S basin margin, the Taleghan fault zone includes two fault strands that bound an intervening sliver (Figure 2). The N strand is principally a high-angle, S dipping reverse fault juxtaposing Triassic-Jurassic Shemshak Formation or Cretaceous limestone against Taleghan basin conglomerate. The S strand is a moderately dipping thrust that places Neoproter-

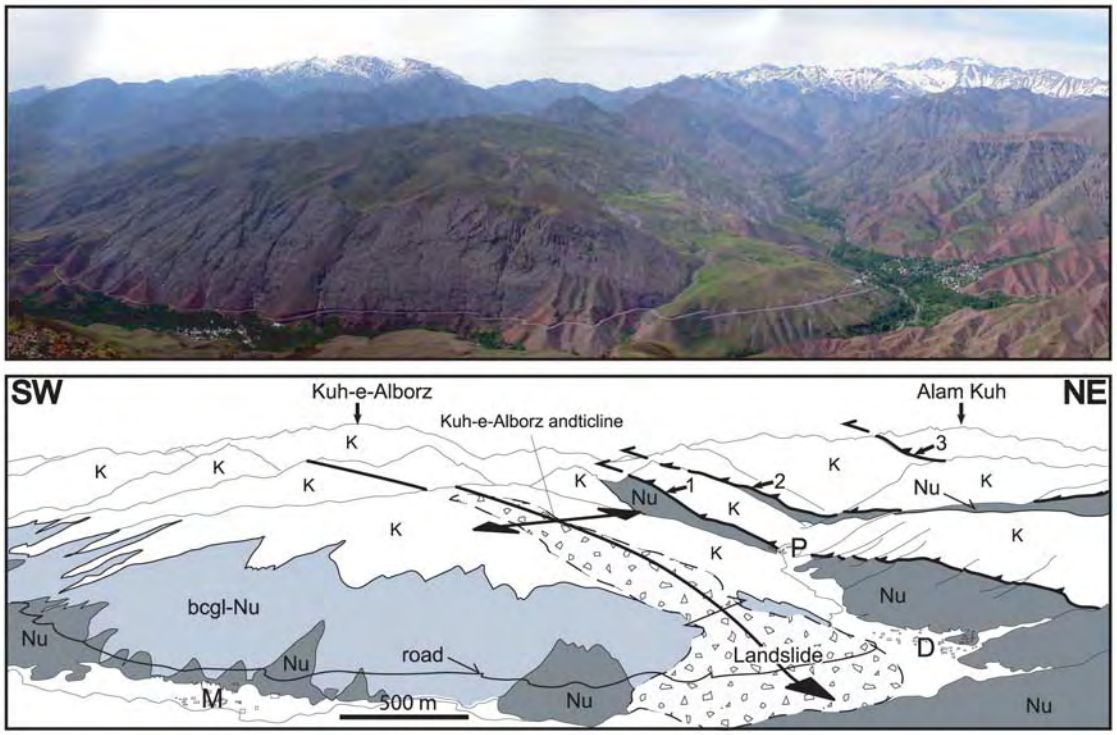

Figure 3. Panorama and line drawing of the E plunging Kuh-e-Alborz anticline in the Taleghan basin. Dark grey shading indicates lacustrine strata of the Narijan unit which rest conformably on a thin veneer of conglomerate (light grey shading) along the S limb of the anticline. K, Karaj Formation (Eocene); Nu, Narijan unit (Miocene); 1, Lower Parachan Thrust; 2, Upper Parachan Thrust; 3, Kandavan Thrust; M, Mehran village; D, Dizan village; P, Parachan village; bcgl, basal conglomerate.

ozoic-Paleozoic rocks over Mesozoic rocks caught between the fault strands. Along the S central margin of the Taleghan basin, the S strand cuts across the N strand, placing Devonian rocks over Taleghan basin conglomerates (Figure 2).

[9] In the easternmost Taleghan basin, sedimentary fill is exposed in footwalls of the SE to E striking upper Parachan, lower Parachan, and Gar Ob thrusts, as well as along the N limb of the Khowchireh anticline (Figure 2). Along the Parachan thrusts, discontinuous exposures of Taleghan basin fill ultimately connect with the Alamut basin (Figure 2). Locally a small exposure of Taleghan basin conglomerate is exposed farther north of the Taleghan syncline in the footwall of the S directed Kandavan thrust.

[10] The SE striking upper and lower Parachan thrusts (Figure 3) dip $\sim$40° NE and generally exhibit dip-slip kinematics. The upper thrust places a hanging wall flat of Karaj Formation on a footwall flat of basal Taleghan strata (Figure 2). The lower Parachan thrust juxtaposes a hanging wall flat of Karaj and basal Taleghan strata over isoclinally folded red siltstone and sandstone of the upper Taleghan succession. From the Alamut river valley in the N, the Parachan fault system is continuous southeastward, truncating the E end of the Taleghan syncline and ultimately merging with the E striking Gar Ob thrust (Figure 2).

[11] At the E limit of the Taleghan basin, the S directed Gar Ob thrust (Figure 2) places a hanging wall flat of Karaj Formation over tightly folded Taleghan basin conglomerates to the south. This fault splays and terminates to the W along the N limb of the Khowchireh anticline but continues eastward beyond the headwaters of the Taleghan river (Figure 2).

[12] The Khowchireh anticline forms the S limit to the Oligocene-Miocene fill of E Taleghan basin, paralleling the Taleghan fault zone to the S (Figure 2). Stream valleys that cut across this anticline expose isoclinally folded Jurassic-Paleocene rocks beneath the Paleocene-Eocene angular unconformity. Growth strata along the N flank of the Khowchireh anticline (Figure 5b) are best exposed near the intersection of the Parachan and Gar Ob thrusts where they overlie in angular unconformity steeply tilted and folded green tuffs of the Eocene Karaj Formation (Figure 2). In places, Gar Ob thrust structures have cut and folded the previously deposited growth strata (Figure 6).

[13] The most significant structure to the N, the ESE striking Kandavan thrust bounds the N edge of the Alamut basin (Figure 2) and approximates the axis of the Alborz. This generally S directed thrust places Paleozoic-Mesozoic rocks over Eocene and younger rocks (Figure 2). The footwall is composed of conglomeratic fill of probable Miocene age that unconformably overlies an Eocene Karaj sequence consisting of black to dark grey shale, turbiditic sandstone, and marl. The Kandavan thrust is cut by the $\sim$6 Ma Alum Kuh granite [*Axen et al.*, 2001].

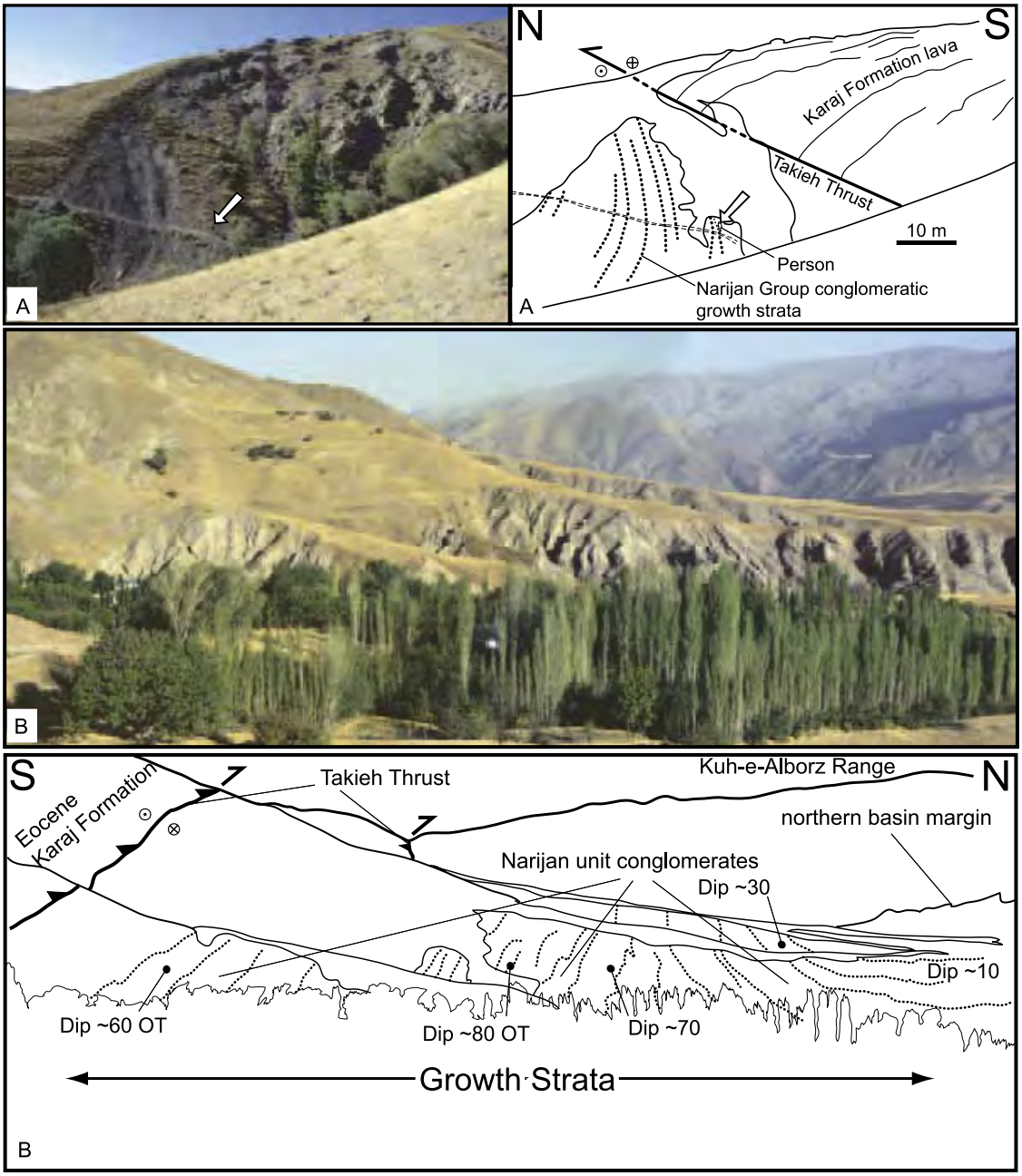

Figure 4. (a) Photograph and line drawing showing the sinistral-reverse Takieh fault of SW Taleghan basin juxtaposing a hanging wall anticline of Karaj Formation (Eocene) lavas over subvertical Narijan unit (Miocene) conglomeratic growth strata. Person for scale. (b) Photograph and line drawing showing Narijan growth strata in the footwall of the Takieh fault. Stratal dip decreases progressively upsection from left to right, from overturned (OT) to upright, indicating tilting during syndepositional displacement along the Takieh thrust.

[14] Estimates of middle to late Cenozoic shortening are poorly constrained owing to earlier episodes of Cretaceous shortening and Eocene extension [*Stöcklin*, 1974; *Berberian*, 1983; *Guest et al.*, 2006b]. Nevertheless, new mapping and a regional cross section suggest a minimum N-S shortening across the Alborz of 36 ± 2 km [*Guest et al.*, 2006a], compatible with an estimate of ~30 km derived from previous syntheses [*Stöcklin*, 1974; *Allen et al.*, 2003].

3. Taleghan Basin

[15] The Taleghan basin consists of two stratigraphic units of Oligocene-Miocene age: the informally named Narijan

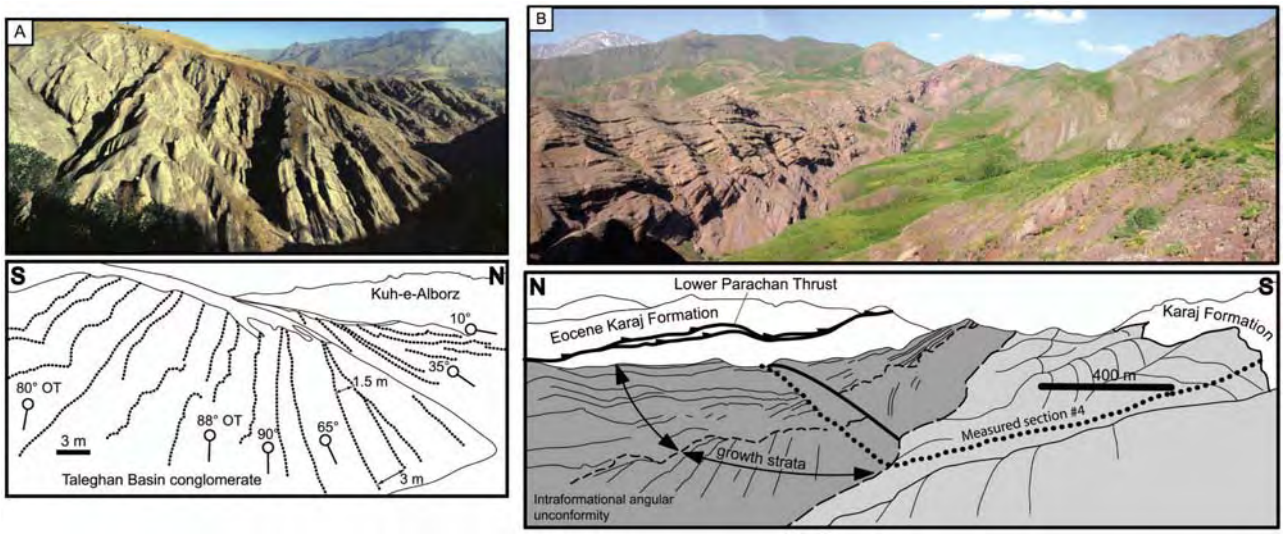

Figure 5. (a) Photograph and line drawing showing growth strata in the Narijan unit (Miocene) in W Taleghan basin. Stratal dip decreases progressively upsection from left to right, from overturned (OT) to upright, attributed to syndepositional displacement along the N vergent Takieh fault ~100 m to left (south) of photo. (b) Photograph and line drawing from E Taleghan basin showing Narijan unit (Miocene) conglomeratic growth strata (dark grey shading) overlying Gand Ab unit (Oligocene) strata (light grey shading). A progressive upsection decrease in bedding dip, from ~70° to ~40°, indicates tilting during syndepositional growth of the Khowchireh anticline to the south, probably in response to reverse slip on the Taleghan and/or Mosha faults.

and Gand Ab units (Figure 7). Measured sections (numbered 1–5 from W to E; Figure 2) are presented in Figure 7. The Narijan unit is exposed throughout the Taleghan basin region whereas the underlying Gand Ab unit is only exposed in the eastern headwaters of the Taleghan river (Figure 2). Separating these two units is a previously unrecognized unconformity.

[16] For the Taleghan basin, $^{40}Ar/^{39}Ar$ results for interbedded, crosscutting, and overlapping igneous rock units constrain the timing of sedimentation and deformation. These analyses involved dating of whole rock (groundmass) material, and in one case hornblende minerals, from basaltic flows, andesitic flows and microdiorite dikes. Analyses were performed at the New Mexico Geochronology Research Laboratory, following methods described by *Heizler et al.* [1999]. Complete results are presented in Tables S1 and S2 in the auxiliary material. Additional age control is provided by a marine fossil assemblage discovered in the Gand Ab unit in SE Taleghan basin.

3.1. Gand Ab Unit

[17] The Gand Ab unit is continuously exposed from the SE to S central part of the Taleghan basin (Figure 2) where it is truncated by the Taleghan fault zone (~2 km SE of Orazan). The Gand Ab unit is 0–400 m thick and grades westward from lacustrine and shallow marine lagoonal facies with thin intercalated basalt flows (near Asekan) to a conglomerate and lava-dominated facies (S of Dizan). Locally, the Gand Ab unit consists of conglomerate overlain by tens to hundreds of meters of lava flows (SW of Kuh-e-Do-Hale, S of Dizan) [*Sieber*, 1970]. The contact between the Gand Ab unit and the overlying Narijan unit is a low-angle angular unconformity (Figure 8).

[18] In the Gand Ab valley (W of Asekan), thin fossiliferous limestone beds crop out 50–70 m upsection of the lava flows. Newly identified marine fossils from these limestones include diagnostic gastropod, coral, and foraminifera species recognized in the Qom Formation farther south [*Schuster and Wielandt*, 1999; *Harzhauser et al.*, 2002]. These species broadly indicate a Rupelian to Burdigalian age, but the presence of coral fossils generally limited to the upper Qom Formation suggests that an Aquitanian to Burdigalian age may be most appropriate [*Schuster and Wielandt*, 1999]. The fossil assemblage supports correlation with the Qom Formation, with the corral fossils suggesting an equivalence to the upper levels of the formation [*Amini*, 1991; *Schuster and Wielandt*, 1999]. The upper Oligocene–lower Miocene Qom Formation consists mainly of marine marl and fossiliferous limestone and is exposed throughout central Iran [*Stöcklin and Setudehnia*, 1977]. It is approximately 1200 m thick near its type section and thins northward to ~50 m near the S front of the Alborz [*Stöcklin and Setudehnia*, 1977].

3.1.1. Gand Ab Volcanic Rocks

[19] Lava flows 100–200 m above the base of the Gand Ab unit range from aphanitic olivine basalt to andesite. In SE Taleghan basin (near Gand Ab), basalts crop out as two individual flow units: an upper 2-m-thick flow yielding an $^{40}Ar/^{39}Ar$ whole rock (groundmass) age of 32.8 ± 0.2 Ma (sample 19-135-1), and a lower 2-m-thick flow yielding an $^{40}Ar/^{39}Ar$ whole rock (groundmass) age of 32.7 ± 0.3 Ma

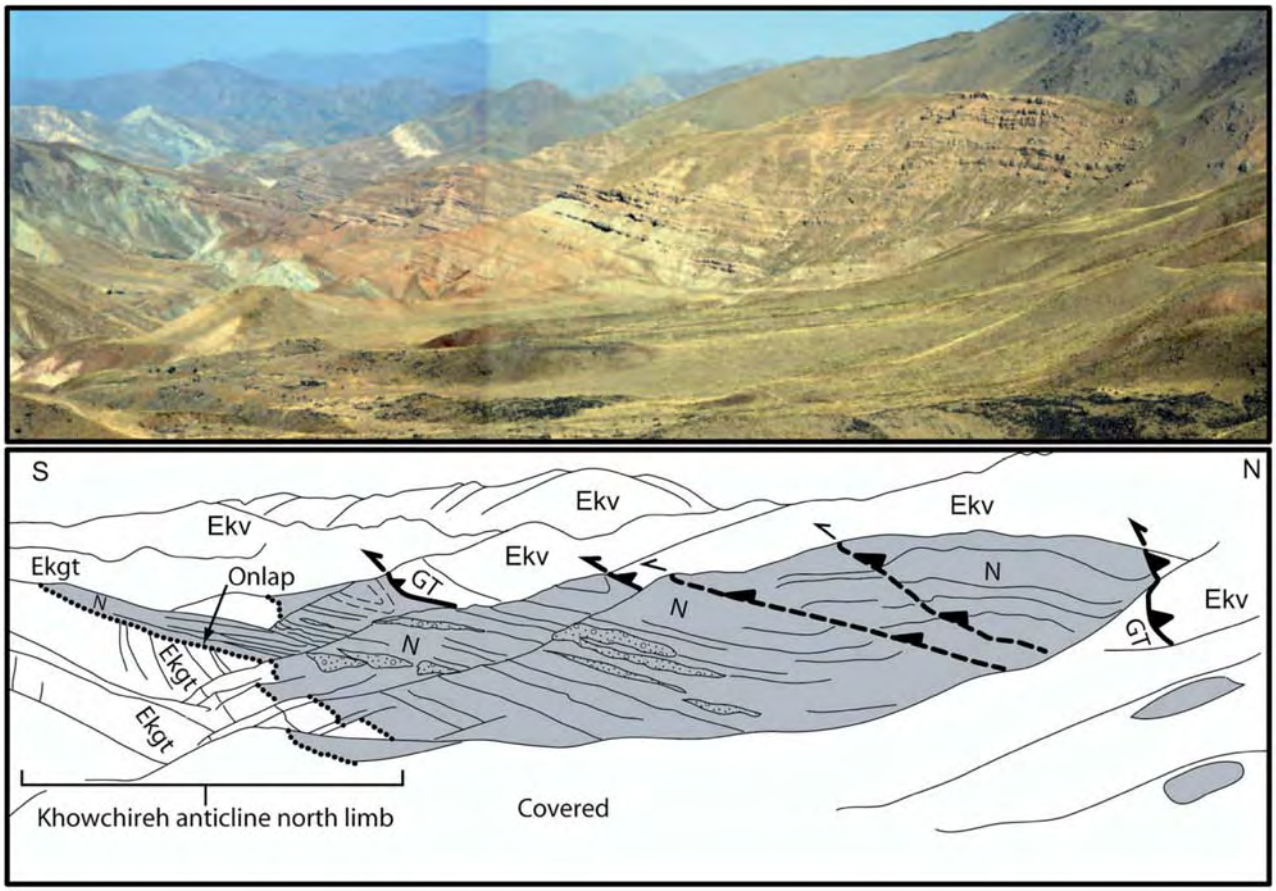

Figure 6. Photograph and line drawing of Narijan unit (Miocene) growth strata lapping southward onto the eroded N limb of the Khowchireh anticline. Rocks of the Karaj Formation (Eocene) are juxtaposed over Narijan unit (N) strata along the Gar Ob thrust (GT). Ekv, Karaj Formation volcanic rocks; Ekgt, Karaj Formation green tuff.

(sample 19-133-1) (Figure 8 and auxiliary material Tables S1 and S2). Both flows have sharp lower boundaries showing limited disturbance of the underlying siltstones and no basal breccia. Within the flow bases, fragments of the underlying red siltstones are preserved. The flow tops are also sharp and lack a well-developed upper breccia. Spring-fed carbonate (travertine) and marl were deposited between the flows. Travertine dikes, which presumably fed the springs, locally cut the lower flow.

[20] In W exposures of the Gand Ab unit, stacked flow units display well-developed brecciated flow tops, commonly with clastic and carbonate strata between flows. In the S central Taleghan basin (near Kuh-e-Do-Hale and to the SW) numerous lava flows exhibiting basal and upper flow breccias compose a succession of stacked basalt and andesite flows several hundred meters thick [*Guest*, 2004].

[21] The dated lava flows place a maximum age limit of 33 Ma on the Gand Ab unit, requiring that all overlying Gand Ab and Narijan strata are Oligocene or younger in age and the 100–200 m of Gand Ab sediment underlying the lava flows is of early Oligocene or possibly latest Eocene age. The relative amount of volcanic material in the succession suggests eruption from vents WSW of the S central Taleghan basin, possibly along the Taleghan fault zone (Figure 7). The two basalt flows in SE Taleghan basin (near Gand Ab; Figure 8) exhibit $^{40}Ar/^{39}Ar$ ages indistinguishable within error, suggesting the sediment between the flows accumulated in a relatively short time.

3.1.2. Sub-Gand Ab Disconformity

[22] The sub-Gand Ab disconformity, exposed in SE Taleghan basin, separates the Gand Ab unit from underlying andesitic lava flows of the Eocene Karaj Formation (Figure 8). The disconformity passes from the S central Taleghan basin (near Orazan), where it has an irregular erosive geometry (with various Gand Ab lava flows and conglomerates capping Karaj lava flows), eastward into a correlative conformity (Figure 2). In E Taleghan basin (near Gand Ab), Karaj lava flows are overlain by Gand Ab marine facies in nonerosive contact with little or no angular discordance (Figure 8). In all other parts of the Taleghan and Alamut basins, the basal Narijan unit rests on the Eocene Karaj Formation implying erosion and/or nondeposition of the Gand Ab unit.

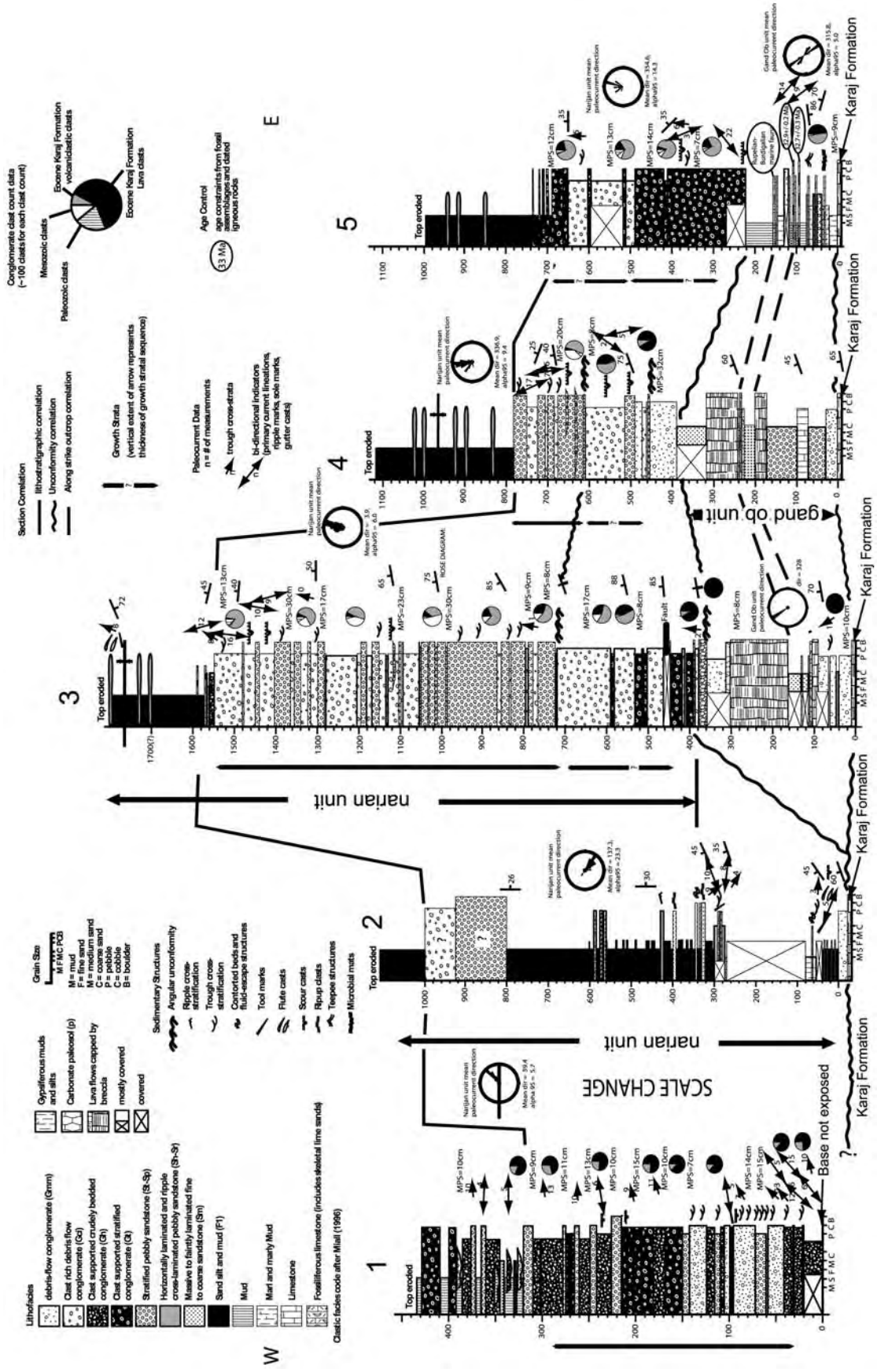
W
E
SCALE CHANGE
narian unit
gand ob unit
Karaj Formation
Base not exposed
Top eroded
Lithofacies
Section Correlation
Paleocurrent Data
Growth Strata
Age Control
Conglomerate clast count data
Sedimentary Structures
Grain Size

Figure 7

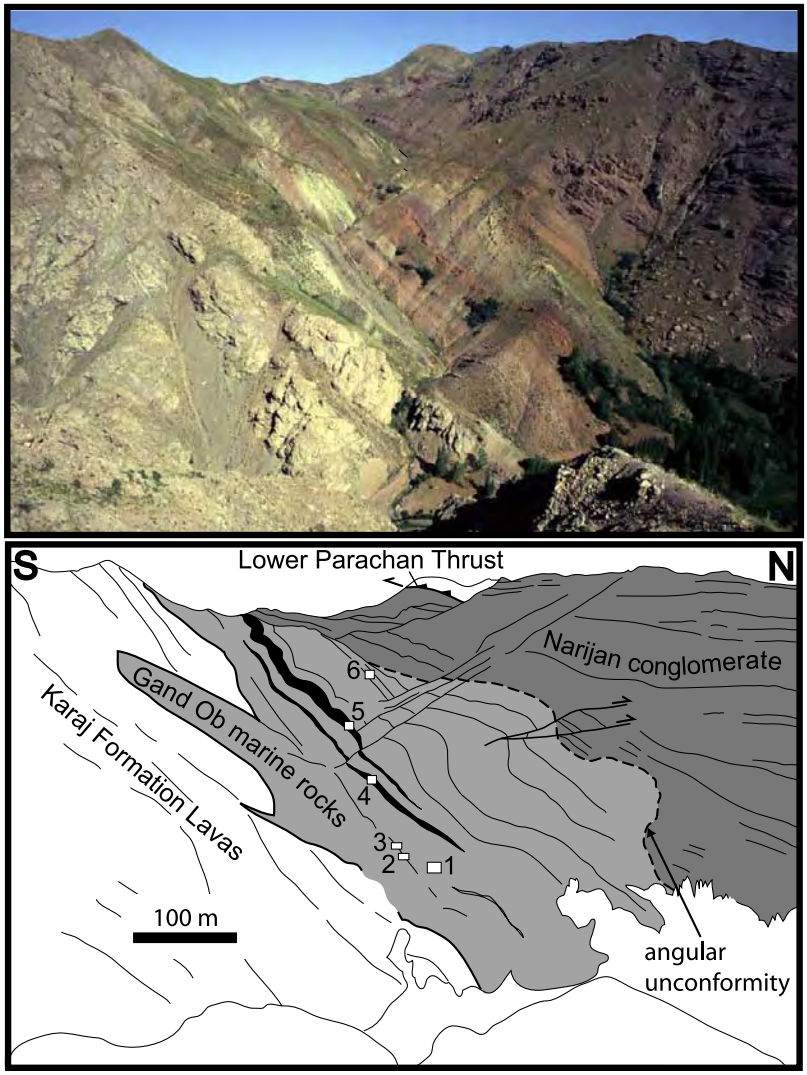

Figure 8. Photograph and line drawing of the Karaj Formation (Eocene) capped unconformably by the Gand Ab unit (light grey shading) and Narijan unit (dark grey shading). Dashed line marks the low-angle angular unconformity between the Gand Ab and Narijan units. Gand Ab lava flows are identified by black shading. Numbers refer to sample localities and photograph localities: 1, location of teepee structure (Figure 11e); 2, location of laminated limestone beds (Figure 11b); 3, location for photos of carbonate structures (Figures 11c and 11d); 4, location of sample 19-133-1 of lower basalt flow (32.7 ± 0.3 Ma); 5, sample 19-135-1 of upper basalt flow (32.86 ± 0.21 Ma); and 6, locality of Rupelian to Burdigalian fossil assemblage.

[23] The age constraints provided above for the middle portion of the Gand Ab unit (32.8 ± 0.2 Ma; 32.7 ± 0.3 Ma) and the late Eocene age for the uppermost Karaj Formation [*Stöcklin*, 1974; *Stöcklin and Setudehnia*, 1977; *Berberian*, 1983] suggest a maximum temporal discordance across the Gand Ab-Karaj contact in the Gand Ab region of ~4 Ma. However, uncertainty about the absolute age of the upper Karaj lava flows suggests that the Gand Ab basalt may have erupted shortly after the final Karaj lavas erupted. This age uncertainty and the lack of an angular discordance suggests a near conformable contact with little or no time missing for the Gand Ab area. This interpretation suggests that deposi-

Figure 7. Measured sections for the Talegan basin displaying facies information, stratigraphic correlations, paleocurrent data (rose diagrams), clast compositional data (pie charts), and fossil sample locations. Lithostratigraphic correlations are defined for the base of the Gand Ab unit, base of the Narijan unit, and abrupt shift to fine-grained facies in the upper Narijan unit. Section locations are shown in Figure 2. See text for descriptions and interpretations of facies and provenance.

tion of the 100–180 m of siltstone, shale, limestone and fine-grained sandstone of the Gand Ab unit stratigraphically between the uppermost Karaj and Gand Ab basalt took place at a rate less than 0.05 mm/yr.

3.2. Narijan Unit

[24] Volumetrically, the Narijan unit comprises most of Taleghan basin. It is preserved in the synclinal keel between the anticlinal Kuh-e-Alborz and Taleghan ranges (Figure 2). The Narijan succession attains a minimum thickness of 400–1400 m and is composed of conglomerate and sandstone with a distinctive uppermost interval dominated by mudstone (Figure 7). The unit is typically folded and contains well-exposed growth strata along the S margin in both the E part (near Narijan) and W part (near Takieh) of the basin (Figures 4–6).

[25] The growth strata exhibit a progressive upsection decrease of dip, individual beds are erosionally truncated by overlying units, and individual bed thicknesses decrease southward toward the Khowchireh anticline in the E (Figure 6) and the Takieh fault in the W (Figures 4 and 5). These growth strata record deposition during progressive tilting of the N limb of the growing fold, similar to stratal geometries documented elsewhere [e.g., *Riba*, 1976; *DeCelles et al.*, 1991; *Ford et al.*, 1997; *Horton*, 1998]. Narijan strata do not match growth triangle geometries formed by kink-band migration and instantaneous tilting of fold limbs [e.g., *Suppe et al.*, 1992, 1997].

[26] The Narijan unit is divided into alluvial fan, braided stream, and lacustrine facies. Red lacustrine siltstone and fluvial sandstone comprise the bulk of the Narijan unit, with alluvial fan conglomerate concentrated along the S margin of the Taleghan basin. Lacustrine strata occur throughout the basin but are concentrated along the synclinal axis and fine toward the N margin of the Taleghan outcrop belt where they are more gypsiferous (Figure 7).

[27] *Annells et al.* [1975b] noted the similarity of the Narijan unit to the Upper Red and Hezardarreh formations of central Iran and tentatively interpreted the Narijan unit as their northern equivalent. The Upper Red Formation conformably overlies the Qom Formation south of the Alborz and has a maximum age of post-Burdigalian based on its position above the Qom [*Stöcklin and Setudehnia*, 1977; *Amini*, 1991]. The minimum age for the Upper Red Formation is poorly constrained, with most estimates suggesting late Miocene, although Pliocene cannot be ruled out [*Stöcklin and Setudehnia*, 1977; *Amini*, 1997; *Davoudzadeh et al.*, 1997]. The Hezardarreh Formation of presumed late Miocene to Pliocene age, which crops out along the S foot of the Alborz, conformably overlies the Upper Red [*Stöcklin and Setudehnia*, 1977] and consists mainly of conglomerate with intercalated sandstone and mudstone in the lower part [*Stöcklin and Setudehnia*, 1977]. The Hezardarreh Formation is ~1000 m thick and generally steeply tilted where exposed. This unit is unconformably overlain by the Quaternary Kahrizak Formation, a subhorizontal, sheet-like alluvial fan conglomerate that extends southward tens of kilometers from the foot of the Alborz [*Rieben*, 1955].

[28] The sub-Narijan unconformity is exposed along the margins of the Taleghan and Alamut basins and locally in the footwalls and hanging walls of various thrust sheets [*Guest*, 2004]. The Narijan unit sits on the Karaj Formation or Gand Ab unit and the contact ranges from nearly concordant to a pronounced angular unconformity (Figure 2).

[29] The sub-Narijan unconformity is an irregular surface that reflects significant local paleo-relief on the erosional surface postdating the Eocene Karaj Formation. Angular discordance between the Karaj and overlying Narijan unit ranges from zero discordance where fluvial and lacustrine facies overlie Karaj lavas to extreme discordance where alluvial fan facies overlie folded and overturned green tuffs of the middle to lower Karaj. Exposures of coarse clastic Narijan facies in angular unconformity above tilted Karaj rocks are best expressed along the N central margin of Alamut basin, the SW margin of Taleghan basin, in the footwall of the NW segment of the lower Parachan thrust, and in the footwall of the Gar Ob thrust along the upper (eastern) Taleghan valley (Figures 2 and 6).

[30] In other areas the sub-Narijan contact is a planar to gently undulatory surface with local breccia and conglomerate filled channels and depressions. In these localities, thin (meter to decimeter scale) gravel lenses separate Karaj lavas from hundreds of meters of fluvial and lacustrine Narijan strata. These contact relationships are identified along the N margin of Taleghan basin (Figure 3), the S margin of Alamut basin, and in footwalls of the central segments of upper and lower Parachan thrusts (Figure 2).

[31] Where the sub-Narijan unconformity lies above the Gand Ab unit, the rocks display 10°–30° of angular discordance, paleo-relief up to ~10 m, discordant paleocurrent directions, and abrupt facies changes. In the S central Taleghan basin (between the Taleghan fault zone near Orazan and ~1 km S of Narijan), the uppermost Gand Ab unit consists of basaltic to andesitic lava and several meters of volcanic agglomerate capped abruptly by the erosional unconformity and overlying massive cobble–boulder conglomerates. In SE Taleghan basin, fluvial and lacustrine facies of the uppermost Gand Ab unit grade rapidly upward into alluvial fan conglomerates of the Narijan unit. In general, Narijan strata directly overlying the Gand Ab unit dip more steeply N than Gand Ab strata (Figure 2). This implies that the Narijan unit, when restored to horizontal, originally overlapped Gand Ab strata that had first been tilted to S dipping orientations.

[32] The temporal discordance across the sub-Narijan unconformity is poorly constrained. In the Gand Ab unit, marine fossils above the lower Oligocene Gand Ab basalt flows (32.8 ± 0.2 Ma; 32.7 ± 0.3 Ma) represent fauna of Rupelian to Burdigalian age, correlative with the Qom Formation of central Iran. The overlying Narijan unit provides no fossil age control. However, the lower Narijan unit was deposited before ~9 Ma on the basis of microdiorite dikes that cut the lower Narijan unit and lower Parachan thrust (~10 km NW of Parachan) and yield $^{40}Ar/^{39}Ar$ whole rock (groundmass) and hornblende ages of 8.74 ± 0.15 Ma, 7.31 ± 0.10 Ma, 7.06 ± 0.08 Ma, and 6.68 ± 0.07 Ma

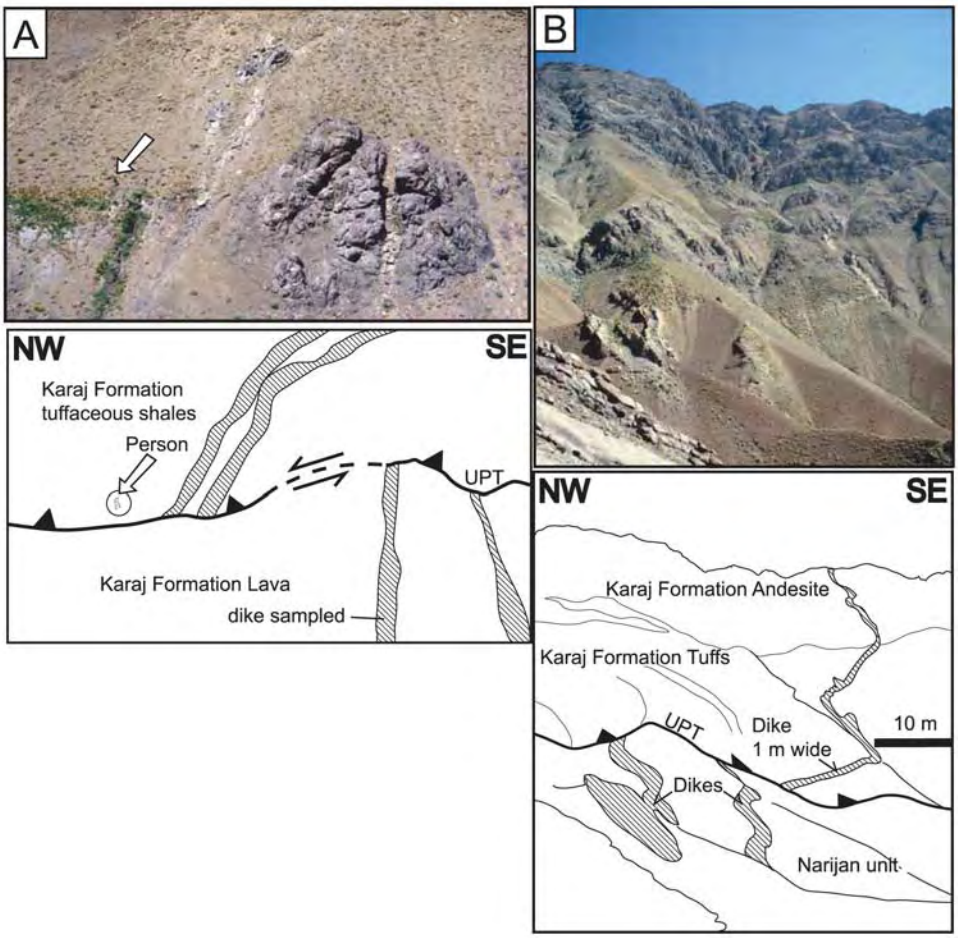

Figure 9. (a) Photograph and line drawing of a dike system cut by the upper Parachan thrust (UPT). The fault places Karaj Formation (Eocene) tuffaceous shales over Karaj lavas and cuts the latest Miocene dikes with <20 m of apparent sinistral offset. (b) Photograph of the upper Parachan thrust (UPT) with dikes intruding hanging wall volcanic rocks of the Karaj Formation and footwall siltstones of the Narijan unit. Dikes display apparent sinistral and dextral offsets along the UPT.

(Figure 9, samples 19-137-1, 4-84-2b, 4-84-2a, and 4-86-3, respectively; Tables 1 and 2). Furthermore, (U-Th)/He detrital apatite cooling ages indicate that the upper and lower portions of the Narijan unit in the Gand Ab area were buried to depths >2 km and then exhumed after 4.7 ± 0.3 Ma to 3.4 ± 0.1 Ma [*Guest*, 2004], suggesting the entire Narijan unit is pre-Pliocene in age. Thus the maximum temporal discordance across the Gand Ab-Narijan unconformity is 20–30 Ma. The minimum temporal discordance across this unconformity is difficult to constrain, and could be less than 1 Ma if tilting, erosion, and a shift in depositional environment occurred rapidly.

3.3. Pliocene–Quaternary Gravel Facies

[33] Pliocene-Quaternary gravels unconformably overlie deformed rocks of the Narijan unit in incised terrace exposures throughout the Taleghan and Alamut basins. We have dated andesitic lava flows capping terraces in Taleghan valley (between Mehran and Johistan) and one lava flow in the S central Alamut basin (Figure 2). One lava flow resting on a paleosurface 300–400 m above the present Taleghan river (a few kilometers SE of Johistan) yields $^{40}Ar/^{39}Ar$ whole rock (groundmass) ages of 2.86 ± 0.83 Ma, 0.46 ± 0.28 Ma, and 0.24 ± 0.03 Ma (sample 3-87, 3-88, and 3-89 respectively; Tables 1 and 2). A smaller exposure (~2 km W of Mehran) yields an $^{40}Ar/^{39}Ar$ whole rock (groundmass) age of 1.40 ± 0.21 Ma (sample 19-57-2; Tables 1 and 2). In the Alamut basin, the lava flow overlies beveled Narijan rocks (near Madan) and yields $^{40}Ar/^{39}Ar$ whole rock (groundmass) ages of 0.31 ± 0.04 Ma (sample 20-49-2) and 0.51 ± 0.06 Ma (sample 20-49-3; Tables 1 and 2).

[34] The new age analyses and crosscutting relationships help constrain the temporal discordance across the basal unconformity. $^{40}Ar/^{39}Ar$ ages for lava flows that rest on the Narijan unit provide a minimum age, and dikes cutting the Narijan unit provide a maximum age. The youngest dike that cuts Narijan rocks and the upper Parachan thrust is

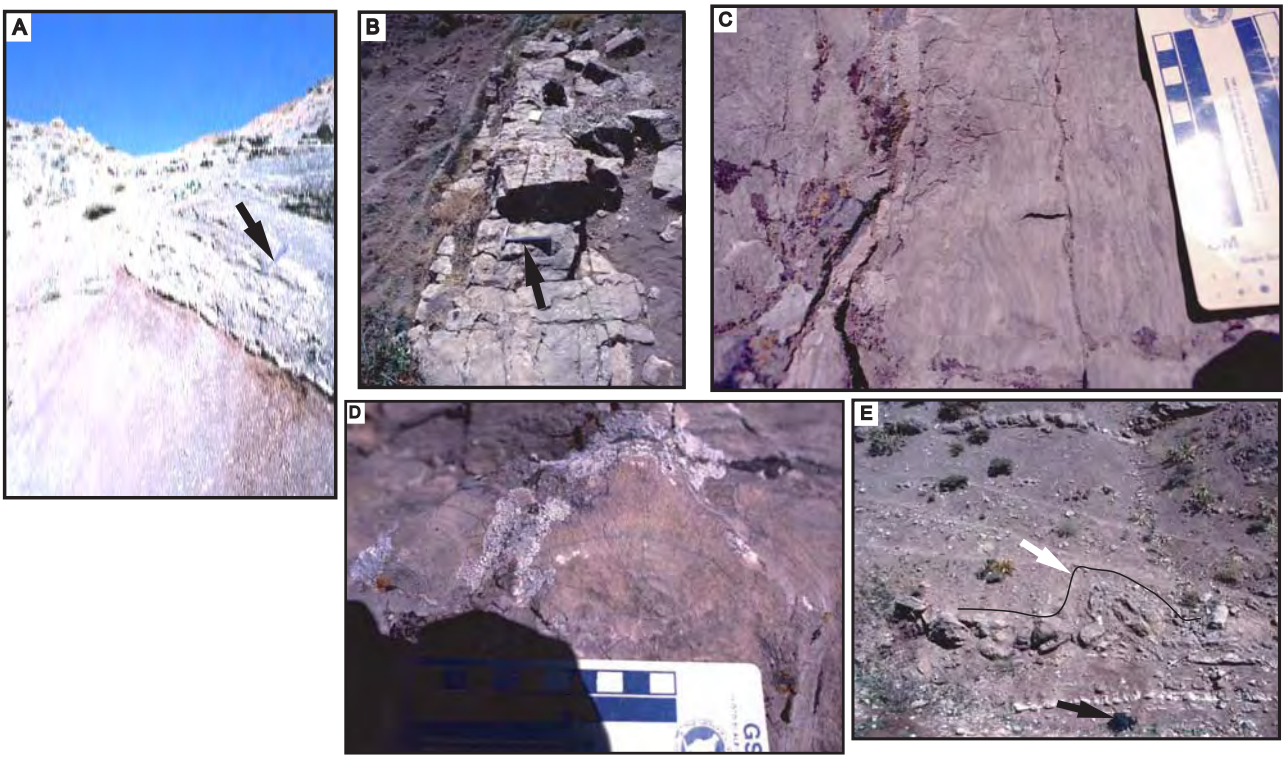

Figure 10. Lagoonal-lacustrine facies association. (a) Red to green silty mudstone with interbedded marl and minor lenticular interbeds of sandstone attributed to subtidal lagoonal or lacustrine deposition. Hammer for scale (arrow). (b) Light grey to blue-grey microbially laminated limestone. Light grey layers are disrupted, fenestral fabrics. Blue-grey layers are intraclastic and pisolithic calcareous sandstones. Hammer is shown for scale (arrow). (c) Limestone with disrupted laminations, intraclasts, and pisoliths. (d) Limestones exhibiting radiating, fan-shaped fibrous calcite hemispheroids. (e) Teepee structure (outlined in black, indicated by white arrow) developed within carbonate bearing mudstones. Note horizontal undisturbed bedding above and below. A ~30-cm waist pack is shown for scale (black arrow).

dated at 6.68 ± 0.07 Ma. This dike was subsequently offset <20 m by the same thrust (Figure 9), implying that most deformation occurred before 6.68 Ma in the Taleghan basin region, with very limited fault displacement thereafter. The oldest age determined for a lava flow above the unconformity is 2.86 ± 0.83 Ma. From these ages, the maximum possible age for the undeformed gravels overlying the unconformity is constrained between the mid-Pliocene (~3 Ma) and latest Miocene (~6 Ma).

4. Taleghan Basin Depositional Systems

[35] Three facies associations characterize the Gand Ab and Narijan units in the Taleghan basin: lagoonal-lacustrine (Figures 10 and 11), alluvial fan (Figure 12), and fluvial (Figure 13) facies associations. The distributions of individual lithofacies are depicted in five measured sections (Figure 7). The following text provides descriptions and interpretations of depositional conditions.

4.1. Lagoonal-Lacustrine Facies Association

[36] This facies association consists of four lithofacies. (1) The most common lithofacies is composed of laminated, violet, red, white, and green mudstone and marl. Beds are tabular, <0.1 m thick, and have nonerosional contacts (Figures 10a, 11a, and 11b). (2) A carbonate lithofacies association consists of decimeter- to millimeter-scale regular to irregularly laminated limestone, micritic limestone, muddy fossiliferous limestone and skeletal calcareous sandstone; these facies are typically interbedded with mudstone and marl (Figure 10b). The laminated limestones exhibit disrupted laminations and well-developed fenestral fabric (Figure 10c). Locally these limestones also contain radiating inorganic growths (Figure 10d). In places, carbonate-filled fracture networks in underlying rocks link into the overlying laminated deposits. Locally evaporitic carbonate forms desiccation (tee-pee) structures overlain by undisturbed siltstone and mudstone (Figure 10e). Laterally continuous micritic limestone beds are massive to laminated and interbedded with mudstone and fine sandstone. Fossiliferous muddy limestone beds are laterally continuous for hundreds of meters and contain marine faunal assemblages. Skeletal calcareous sandstone is composed of broken shell fragments cemented by white calcareous micrite. (3) A third, less common lithofacies consists of fine- to coarse-grained, rarely pebbly, massive- to reverse-graded sandstone

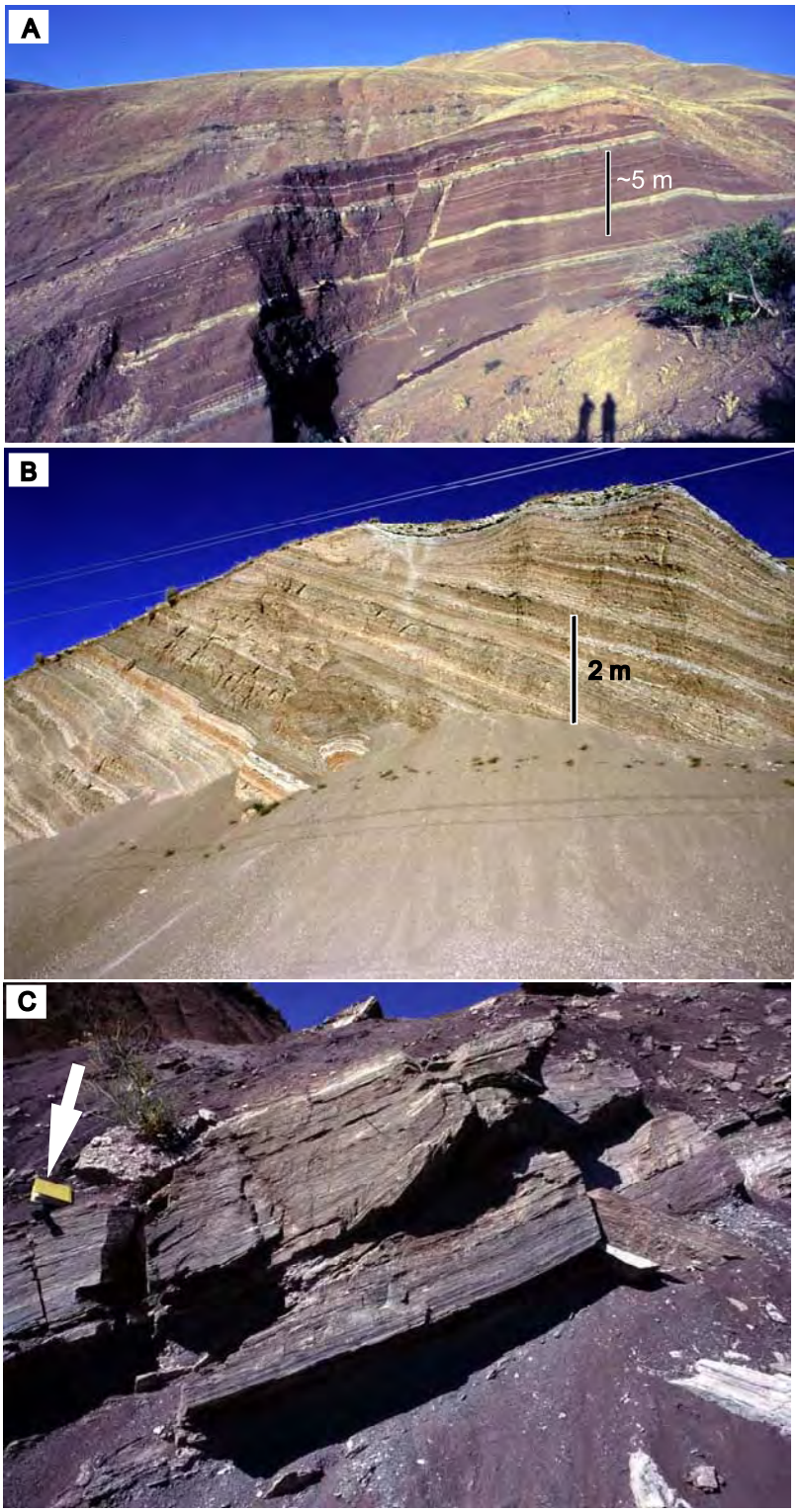

Figure 11. Lacustrine facies association. (a) Red silty mudstone facies with interbedded white gypsum layers. (b) Brown to tan mudstone facies interbedded with white to pink gypsum. (c) Laminated gypsum interbedded with grey claystone and red silty mudstone. Field notebook (12 × 19 cm) is shown for scale (arrow).

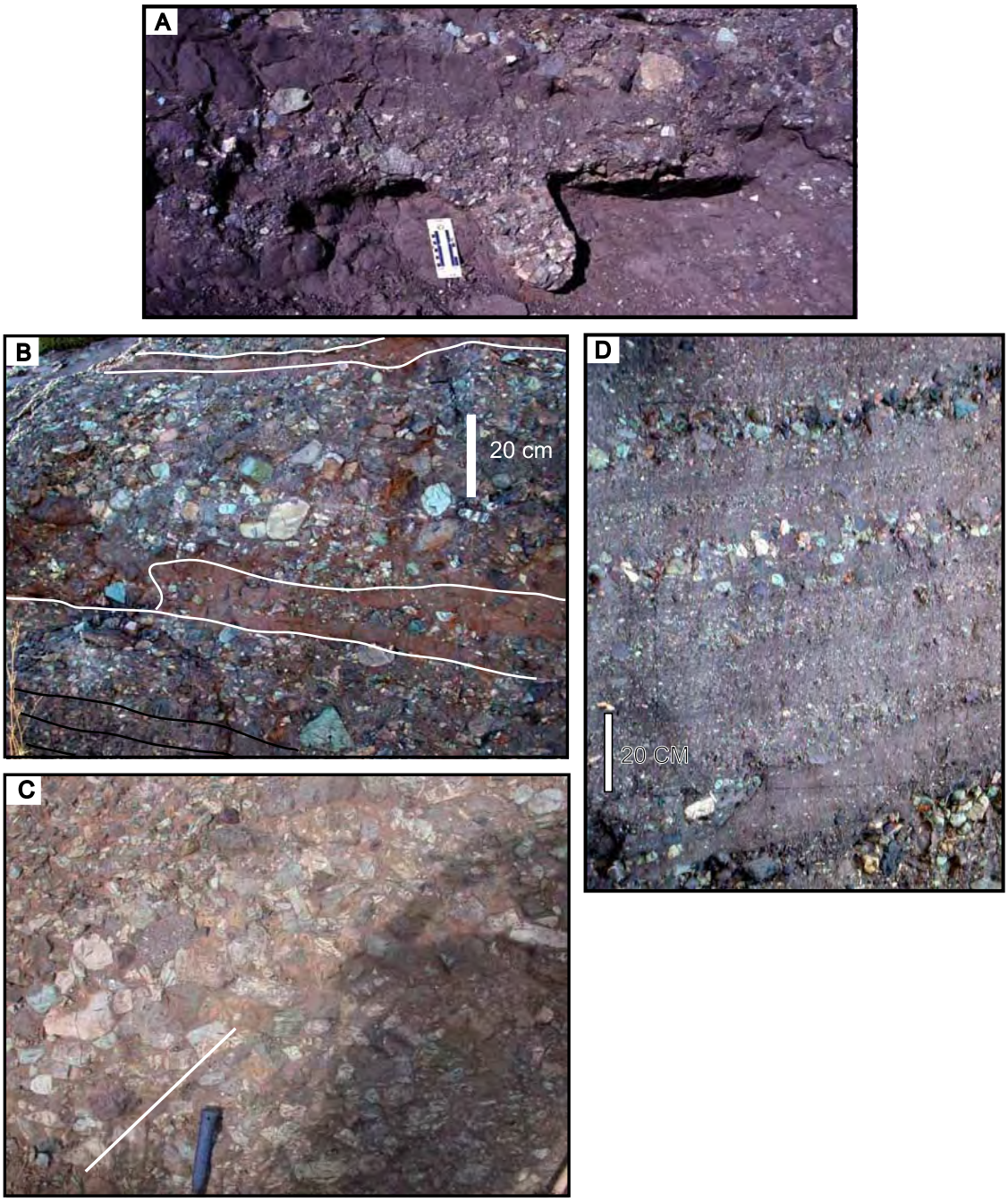

Figure 12. Alluvial fan facies association. (a) Clast-supported crudely stratified, normally graded conglomerate with scoured base (Facies Gh). Note deep gutter cast cut into underlying sandstone. (b) Stratified conglomerate (Facies Gt) sharply interstratified with pebbly sandstones (white lines indicate contact; black lines indicate stratification in conglomerate). (c) Reverse and normally graded clast supported conglomerate (Facies Gci). White line parallels bedding. Hammer handle is shown for scale. (d) Cross-stratified and planar-stratified gravelly sandstones (Facies St and Sp) exhibiting basal scours. Note interstratified pebble–cobble conglomerate lenses.

(Sm, Figure 7). Beds are 0.5 to 3 m thick, commonly with flat, rarely irregular, bases, and are laterally continuous for tens of meters. Beds commonly contain mud rip-up clasts oriented with long axes parallel to bedding contacts. Local pebbly beds exhibit reverse grading with pebbles supported in a sandstone matrix. Soft-sediment deformation is common. Traction-transport structures include horizontal to ripple cross-stratification and soft-sediment deformation is

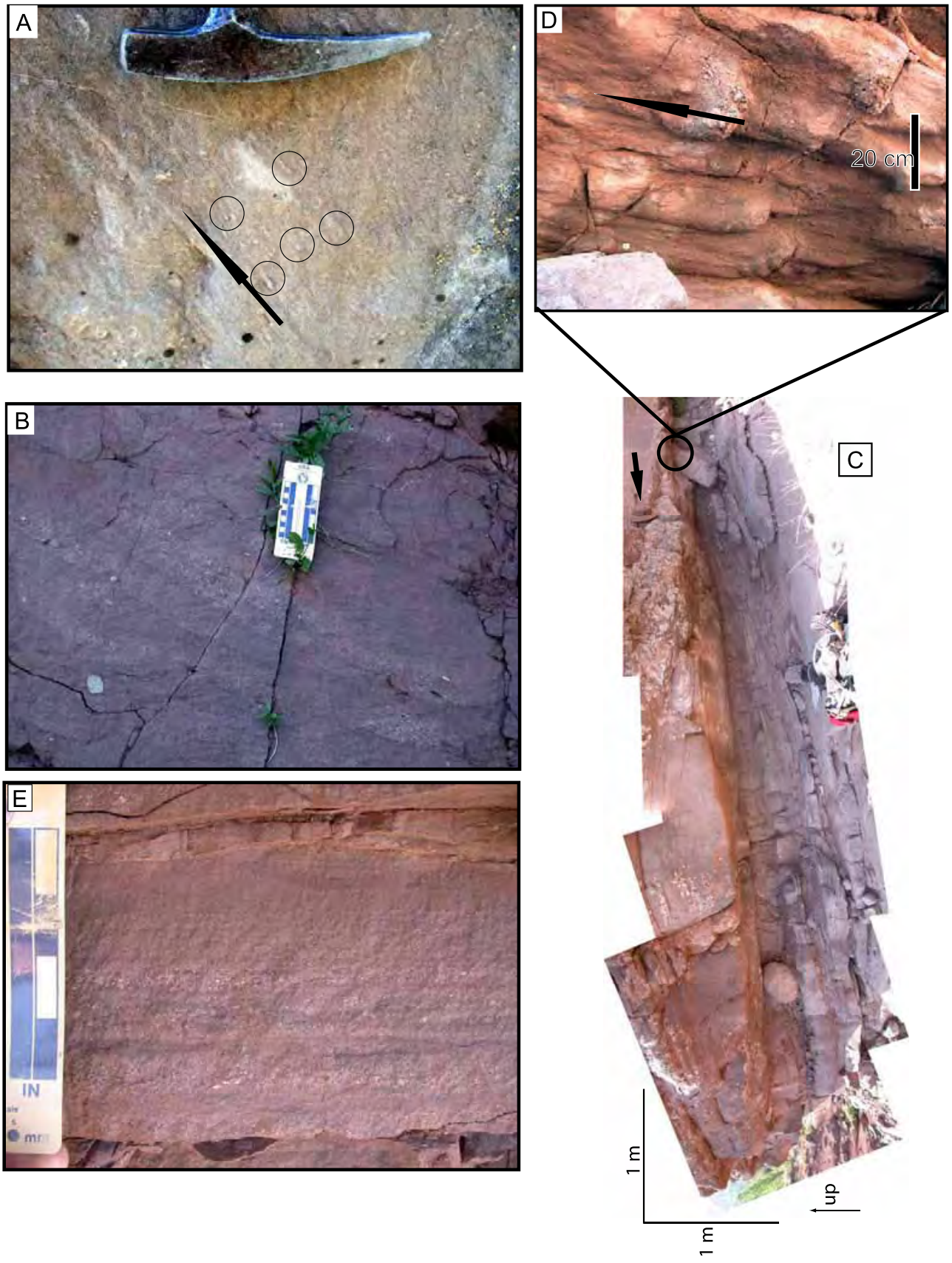

Figure 13

common. (4) The gypsum lithofacies is limited to mudstone-dominated intervals (Figure 11). Beds are 0.01 to 1 m thick and typically exhibit centimeter- to millimeter-scale horizontal laminations. Crystalline and popcorn gypsum occur locally.

[37] Rocks of the lagoonal-lacustrine facies association are interpreted to be the products of suspension fallout, turbidity currents, wave-induced currents, carbonate precipitation in lakes or shallow seawater, and gypsum precipitation during short-lived desiccation episodes. (1) Massive to laminated mudstones represent deposition by suspension fallout [*Ghibaudo*, 1992]. This occurred in lacustrine environments when suspended mud entered the water column as turbidity currents [e.g., *Weirich*, 1989; *Mohrig et al.*, 1998]. Alternatively, this fine-grained facies may have been deposited by periodic sheetflooding events in fluvial floodplains or playas [e.g., *Hampton and Horton*, 2007]. (2) Of the various carbonates, irregular to regularly laminated, internally disrupted limestones with fenestral fabrics are interpreted as low-energy intertidal carbonates where microbial mats flourished [*James*, 1984]. Marl, skeletal calcareous sandstone, and fossiliferous limestone are interpreted as subtidal lagoonal facies [*James*, 1984]. Some thin carbonate beds interbedded with mudstones may be of evaporitic origin [e.g., *Tucker*, 1978]. (3) We attribute massive sandstones to rapid deposition of suspended sand in turbidity currents [*Lowe*, 1982]. Horizontal to ripple cross-stratified sandstone represents bed form growth and migration, probably in turbidity currents [*Lowe*, 1982; *Ghibaudo*, 1992] or wave-induced currents in shallow water [*Horton and Schmitt*, 1996]. (4) Thin beds of laminar and nodular gypsum within mudstone sequences are interpreted as evaporites. Laminated and popcorn gypsum precipitated in shallow water whereas thicker crystalline gypsum beds precipitated in deeper water [*Kendall*, 1984].

4.2. Alluvial Fan Facies Association

[38] Conglomeratic sections 300 to 1500 meters thick are localized along the S margin of Taleghan basin (Figure 2). Four lithofacies comprise this facies association. (1) The first lithofacies consists of moderately sorted, crudely planar-stratified, sandy pebble–boulder conglomerate (Gh, Figure 7). Angular to rounded clasts occur in reverse and normally graded beds that are 0.1 to 3 m thick and laterally discontinuous. Beds have irregular erosional bases exhibiting gutter casts and channel scours (Figure 12a). Relief on basal contacts can exceed 1 m. Sandy interbeds are common in coarser sections whereas lenticular pebble–boulder beds are common in sandy sections. (2) A second lithofacies consists of planar-stratified and trough cross-stratified pebble–cobble conglomerate (Gt, Figure 7). Beds are laterally continuous for tens of meters, 0.5 to 1 m thick, and are interstratified with 0.1- to 0.5-m-thick sandstone beds (Figure 12b). Contacts between sandstone and conglomerate beds are sharp and planar. (3) A third lithofacies consists of poorly sorted, massive to weakly planar-stratified, matrix-supported (Gmm, Figure 7) and clast-supported (Gci, Figure 7) granule-cobble conglomerate (Figure 12c). Weakly stratified beds are 0.5 to 1.5 m thick whereas massive beds are commonly >1 m thick. Beds are laterally continuous for tens of meters and have flat to gently irregular bases. (4) A fourth lithofacies consists of gravelly, medium-grained to granular sandstone and pebble–cobble conglomerate (St and Sp, Figures 7 and 12d). Beds are 0.5 to 5 m thick, commonly exhibit well-developed trough and planar cross stratification and have gently irregular bases.

[39] These lithofacies indicate deposition in a medial to proximal alluvial fan environment with a combination of water flow and debris flow processes. (1) Planar-stratified, clast-supported conglomerates (Gh) are interpreted as longitudinal bar or lag deposits [*Miall*, 1996]. (2) Planar-stratified and trough cross-stratified pebble–cobble conglomerate (Gt) interstratified with sandstones are interpreted as deposits of confined water flows in small channels and unconfined sheetflows across the fan surface [e.g., *Blair*, 1986; *Hampton and Horton*, 2007]. (3) Matrix-supported massive conglomerates (Gmm) and normally to inversely graded, clast-supported conglomerate (Gci) are interpreted as plastic debris flows and clast-rich debris flows, respectively [e.g., *Shultz*, 1984]. Alternatively, graded conglometate (Gci) could be interpreted as hyperconcentrated flow deposits [*Smith*, 1986]. (4) Planar and trough cross-stratified, medium- to coarse-grained pebbly sandstones (St and Sp) are interpreted as remnants of 3-D sinuous-crested and linguoid dunes (trough cross strata) and as 2-D transverse and linguoid dunes (planar cross strata). The high concentration of gravel material common in these deposits suggests a water velocity >1 m/s [*Harms et al.*, 1982; *Ashley*, 1990].

4.3. Fluvial Facies Association

[40] Sandstones occur as thin lenticular bodies within the mudstone-dominated successions of the central and E Taleghan basin (Figure 2). Five lithofacies comprise this facies association. (1) The most common fluvial lithofacies consists of very fine to coarse-grained, rarely pebbly, horizontal to ripple cross-laminated sandstone (Sr and Sh). The beds extend laterally for tens of meters, and typically have individual bed thicknesses of 1–50 cm arranged in lenticular stories several meters thick. Basal contacts are sharp and commonly exhibit parting lineations and crescent scours (Figure 13a). (2) A second lithofacies (St and Sp) consists of fine- to coarse-grained, commonly pebbly, planar and trough cross-stratified sandstone (Figures 13b and 13c). Beds of this facies are lenticular, 1 to 3 m thick, and

Figure 13. Fluvial facies association. (a) Planar-stratified pebbly sandstone (Facies Sr and Sh) with parting lineations and crescent scours (circled). Arrow indicating paleoflow direction. Hammerhead is shown for scale. (b) Trough and planar cross-stratified, fine- to medium-grained, pebble sandstones (Facies St and Sp). (c) Lenticular sandstone body exhibiting large trough and planar cross-strata (Facies St and Sp). (d) Large flute casts on the underside of preserved channel shown in Figure 14c. Paleoflow direction is shown by black arrow. (e) Thinly laminated, laterally continuous, decimeter-scale siltstone beds (Facies Fl) with interbedded thin sandstones.

laterally continuous for tens of meters. Beds commonly rest in broad channels and exhibit erosive bases with flute casts and tool marks (Figures 13c and 13d). Internal soft-sediment deformation is common. (3) The fourth lithofacies (Fl) consists of sandy siltstone. Beds are 0.05 m to 0.3 m thick and laterally continuous for tens of meters. Beds also exhibit sharp, regular contacts and have fine laminations and rare ripple structures (Figure 13e).

[41] This facies association represents fluvial channel and overbank depositional environments. (1) Pebbly sandstones with ripple cross lamination (Sr) and planar lamination (Sh) were deposited in lower flow regime and upper plane-bed flow conditions. The lower flow regime rippled facies are associated with shallow water in abandoned channels and pools where temporary vortices are induced by wind action or by sporadic inflow from the active channel [*Miall*, 1996]. (2) Planar (Sp) and trough cross-stratified (St), medium- to coarse-grained, pebbly sandstones are interpreted as stream channel deposits where 2D and 3D dunes developed in water flowing at approximate velocities of ~0.4 to 1.5 m/s [*Cant*, 1978]. (3) Thin beds of silt with subordinate sand (Fl) are interpreted as flood overbank deposits where material is deposited as suspension fallout and in weak traction currents on the floodplain adjacent to the main channel [*Miall*, 1996; *Hampton and Horton*, 2007].

5. Taleghan Basin Provenance

5.1. Paleocurrents

[42] Sediment dispersal directions for the Gand Ab and Narijan units are plotted on the measured sections (Figure 7) to show mean directions (arrows) and internal variability (rose diagrams). Measured unidirectional indicators include trough axes and trough limbs; bidirectional indicators include parting lineations, ripple marks, flute casts, and tool marks. Paleocurrents in the Gand Ab unit, exposed in measured section 5, indicate NW or SE oriented flow, subparallel to bedding strike (Figures 2 and 7). However, because the Gand Ab unit displays a rough eastward change from proximal clastic and volcanic rocks to more distal marine facies, the paleoflow direction in the Gand Ab unit is considered to have been generally toward the SE. Gand Ab paleocurrent indicators are rare in measured sections 3 and 4 owing to insufficient exposure. Measured section 4 has a single measurement of NW directed flow.

[43] In the Narijan unit, paleocurrent indicators from conglomeratic alluvial fan facies (Figure 7, measured sections 1, 3, 4, and 5) suggest paleoflow directions to the NNW and NE, whereas those from the fluvial and lacustrine facies (Figure 7, measured section 2) generally suggest NW-SE oriented paleocurrents. In the conglomeratic facies, paleoflow was roughly parallel to the present NNE dip of bedding (Figure 2). In the fluvial and lacustrine facies, paleoflow was commonly subparallel to NW-SE bedding strike.

5.2. Conglomerate Clast Composition

[44] Conglomerate clast counts were conducted in measured sections by outlining a 1 × 1 m outcrop area and counting all visible clasts >1 cm. On average, each clast count identified ~100–150 clasts. Our mapping experience in the surrounding region [*Guest*, 2004; *Guest et al.*, 2006a] allowed us to confidently group clasts into four categories: Karaj lavas, Karaj sedimentary rocks, Mesozoic rocks, and Paleozoic rocks. In the Gand Ab unit, clast populations of conglomerates range from 100% Karaj lava clasts in section 3 to 50% Karaj lava and 45% Karaj sedimentary clasts in section 5 (Figure 7). Poor exposure, however, limited the number of clast counts for the Gand Ab unit.

[45] In the Narijan unit the clast population in measured sections 3, 4, and 5 changes upsection from nearly 100% Karaj lava clasts at the base to more than 50% Karaj sedimentary clasts and <10% Mesozoic (Tiz Kuh Orbitolina limestone) and Paleozoic clasts (Kahar quartzite, Lalun sandstone, and Soltanieh and Mila dolomite) near the middle of the section (Figure 7). Clasts in the upper portions of measured sections 3, and 4 are dominated by Mesozoic rocks and Karaj sedimentary rocks with subordinate clasts of Paleozoic rocks and Karaj lavas comprising <20% combined (Figure 7). The upper portion of measured section 5 consists mainly of Karaj sedimentary clasts with the Karaj lava and Paleozoic clasts comprising ~25% combined (Figure 7).

[46] The Narijan unit in measured section 1, located in W Taleghan basin, has a fairly uniform clast distribution throughout the section. From the base to the top of this ~400 m stratigraphic section the clast composition remains ~75% Karaj lavas and ~25% Karaj sedimentary rocks (Figure 7).

5.3. Provenance Interpretation

5.3.1. Gand Ab Unit

[47] Although clast count results are limited for the Gand Ab unit, we tentatively attribute the clast variation between sections 3 and 5 to differences in the size of source drainage networks. The proximal, pebble–cobble-conglomerates of section 3 were potentially derived from a relatively small drainage network composed of Karaj lavas. In contrast, the distal, sandy pebble conglomerate with interstratified marine strata in section 5 may have been derived from a larger drainage network in which the entire Karaj and limited older formations were exposed.

[48] The lateral facies change in the Gand Ab unit from marine strata in the E to proximal nonmarine clastic facies in the W and the NW to SE paleoflow direction suggest a sediment source area roughly west of the Taleghan basin. Moreover, westward thickening of the Gand Ab lava flows, from hundreds of meters in measured section 3 to >1000 m at the point where the Gand Ab unit is truncated by the Taleghan fault zone (Figure 2), implies an igneous source to the W, possibly in the central Taleghan range where several intrusive outcrops have been mapped [*Annells et al.*, 1975a, 1975b, 1977].

5.3.2. Narijan Unit

[49] Clast counts for the Narijan unit in measured sections 3, 4, and 5 exhibit a clear unroofing sequence (Figure 7) indicative of progressive exhumation. A southern source area is suggested by N directed paleocurrents for the Narijan

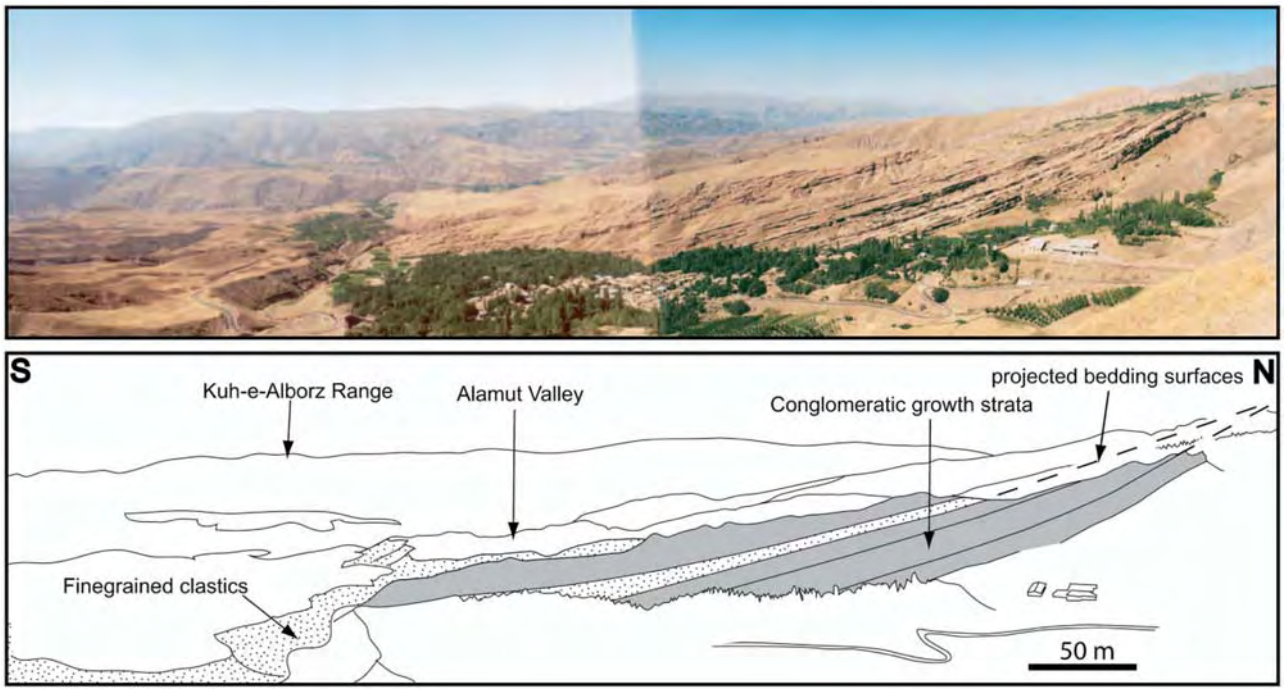

Figure 14. Photograph and line drawing showing conglomeratic section exposed along the N margin of the Alamut basin. When bedding is projected, the succession appears to thin northward toward the Kandavan thrust (<1 km to the right), suggesting a growth stratal relationship. The conglomerates pass laterally into fine-grained rocks to the south (left), which are concentrated along the S margin of the Alamut valley in the distance.

unit and growth strata indicating syncontractional deposition above a large structure south of exposed Taleghan basin fill. The origin of the Narijan unit in these sections is thus attributed to structural growth and progressive unroofing of the Taleghan range (Figure 2).

[50] For section 1 in SW Taleghan basin, Narijan clast counts indicate a source region where only Karaj Formation was exposed. The presence of paleocurrent indicators indicating NE paleoflow and Narijan unit growth strata in the footwall of the Takeih thrust suggest a source region in the northern Qazvin range, located in the hanging wall of the Takieh thrust SSW of W Taleghan basin (Figure 2). Accordingly, the northern Qazvin range is situated directly north of the westernmost Taleghan range and is composed of Karaj rocks (Figure 2).

[51] Measured section 2 displays E-W paleocurrent indicators for the Narijan unit. We interpret these data to indicate an axial drainage system (generally fluvial, but lacustrine at times) oriented roughly perpendicular to the alluvial fan drainage systems located along the deforming margins of the basin.

6. Alamut Basin

[52] Although not the focus of this study, information regarding the structure and sedimentary rocks of Alamut basin, located northwest of Taleghan basin, is important for a reconstruction of deformation and basin development in the western Alborz. Information reported here comes from reconnaissance field work and maps and reports from the Geological Survey of Iran.

[53] The Alamut basin is bounded along its S margin by the anticlinal Kuh-e-Alborz range and along its N margin by the S directed Kandavan thrust (Figure 2). Along the N margin, the Kandavan sheet is composed mainly of Neoproterozoic and Mesozoic sedimentary rocks in thrust contact over extensive outcrops of Eocene Karaj volcanic rocks [*Annells et al.*, 1977]. Along the S basin margin, the contact between the Alamut basin fill of probable Oligocene-Miocene age and the Eocene Karaj Formation varies along strike from a high-angle reverse fault at the E limit of the basin to a depositional contact along the central part of the basin [*Annells et al.*, 1977]. Farther west, the Alamut-Karaj contact remains depositional along the W edge of Alamut basin [*Annells et al.*, 1975a]. On the E edge of the Alamut basin, rocks are cut by the upper and lower Parachan thrusts which apparently die out along strike to the WNW (Figure 2).

[54] The N margin of Alamut basin is dominated by conglomeratic deposits, including outcrops tentatively interpreted as growth strata (Figure 14). Alamut conglomerates occur in beds that are laterally continuous for hundreds of meters and are composed of clasts of carbonate and Karaj lavas. The central and S Alamut basin is dominated by

fluvial and lacustrine facies, including evaporite deposits [*Annells et al.*, 1975a, 1975b]. The contact between Alamut lacustrine strata and underlying Karaj tuffaceous rocks at the E end of the basin is mapped as a high-angle reverse fault that dies out west of a lava flow near Madan [*Annells et al.*, 1975a, 1975b]. Reconnaissance work in this region indicates that the contact is a steeply dipping unconformity with Karaj lavas overlain by a thin sequence of Alamut conglomerates and siltstones that is, in turn, overlapped by the subhorizontal Madan lava flow.

[55] The structure and sedimentology of the Alamut basin bears a mirror-image resemblance to the Taleghan basin. The possible growth strata that dominate the N part of the Alamut basin become progressively thinner and coarser northward. These conglomeratic strata are considered to represent alluvial fans derived from sources north of the Alamut basin. This interpretation implies surface uplift to the N, probably related to Miocene slip on the Kandavan thrust. In contrast, the fine-grained clastic and evaporitic rocks exposed along the central and S Alamut basin were probably deposited in axial fluvial and lacustrine environments.

[56] Alamut strata can be traced farther ESE in the footwalls of the upper and lower Parachan thrusts until they ultimately merge with the Narijan unit exposed in E Taleghan basin. We therefore interpret strata of Alamut basin as belonging to the Narijan unit of Taleghan basin. This interpretation indicates former linkage of the Taleghan and Alamut basins, suggesting they are preserved remnants of a single larger basin that we refer to as the ancestral Taleghan-Alamut basin.

7. Basin Development

[57] Paleogeographic reconstructions of depositional systems and sediment dispersal patterns indicate three phases of basin evolution in the Taleghan-Alamut basin system: (1) a preorogenic phase involving shallow marine to lagoonal deposition and mixed fluvial and alluvial fan deposition of the Gand Ab unit in E Taleghan basin (Figure 15a); (2) synorogenic alluvial fan, fluvial, and lacustrine deposition of the Narijan unit in Taleghan and Alamut basins (Figure 15b and Figure 17 in section 7.2); and (3) progressive synorogenic deformation and structural partitioning of the ancestral Taleghan-Alamut basin system (Figure 17 in section 7.2).

7.1. Phase 1: Deposition of Gand Ab Unit

[58] Lithofacies similarities and a diagnostic marine fossil assemblage in the Gand Ab unit of the E part of Taleghan basin confirm a correlation to the upper Oligocene–lower Miocene Qom Formation carbonates south of the Alborz. Along with independent $^{40}Ar/^{39}Ar$ age control for interbedded lava flows, this lithostratigraphic correlation demonstrates a spatial linkage to the late Oligocene–early Miocene interior seaway of central Iran. The observed lagoonal-lacustrine facies and westward pinchout of marine rocks in the Taleghan basin further suggest deposition in an isolated marine lagoon or embayment along the northernmost edge of the seaway (Figure 15a). Although significant, the marine facies are subordinate to fluvial-lacustrine and alluvial fan deposits in the Gand Ab unit. These deposits and local alluvial fan deposition exhibit facies trends and provenance signatures indicative of a proximal sediment source area along the W margin of the Taleghan basin.

[59] On the basis of $^{40}Ar/^{39}Ar$ isotopic age data for interbedded volcanic rocks, the maximum age for the Gand Ab unit is early Oligocene or possibly latest Eocene. The minimum age for this facies is Burdigalian (20.4 to 16.0 Ma), an estimate provided by a new fossil assemblage and correlation with the Qom Formation of central Iran.

7.2. Phase 2: Deposition of Narijan Unit

[60] Extensive alluvial fan, fluvial, and lacustrine sedimentation characterized deposition of the Narijan unit in the Taleghan and Alamut basins. Along the S margin of the Taleghan syncline, a 400- to 1000-m-thick sequence of Narijan alluvial fan growth strata is continuous along strike and therefore probably formed a series of overlapping fans (i.e., bajada) that sloped northward, eventually terminating in axial fluvial and lacustrine environments (Figure 15b). The more-distal fluvial and lacustrine facies are concentrated on the N limb of the Taleghan syncline and shared S limb of the Kuh-e-Alborz anticline (Figures 2 and 3).

[61] In the Alamut basin hundreds of meters of conglomerate with probable growth strata are exposed along the N margin of the Alamut syncline and pass southward into axial fluvial and lacustrine environments (Figure 14). Lacustrine rocks are concentrated along the axis and S side of the syncline, adjacent to the N limb of the Kuh-e-Alborz anticline (Figures 2 and 3). Fluvial and lacustrine rocks are exposed along the Parachan thrust system from Taleghan basin to Alamut basin (Figure 2). We interpret these to be fragments of the Narijan unit, thereby establishing a depositional link between strata of the Alamut and Taleghan basins.

[62] We correlate the Alamut basin fill with the Narijan unit of Taleghan basin and propose that these basins are preserved remnants of a larger ancestral Taleghan-Alamut basin (Figure 16a). Therefore the N edge of the Alamut basin and S edge of the Taleghan basin represent the ancestral Taleghan-Alamut basin margins. The basin fill preserves facies that record the spatial transition from alluvial fan and fluvial depositional environments along the original basin margins to a lacustrine depositional system in the center of the ancestral Taleghan-Alamut basin (Figure 16b). The development of the Kuh-e-Alborz anticline resulted in the uplift and erosion of the original basin axis, thereby partitioning the basin into the isolated Alamut and Taleghan basins (Figure 17).

[63] The upsection transition from alluvial fan to fluvial-lacustrine facies suggests a change in depositional pattern, climate, and/or structural configuration of the ancestral Taleghan-Alamut basin. During deposition of the lower and middle Narijan unit, the basin contained multiple alluvial fans along its margins and an axial fluvial or lacustrine system dominating the basin center. However, upper Narijan facies indicate that the alluvial fans retreated

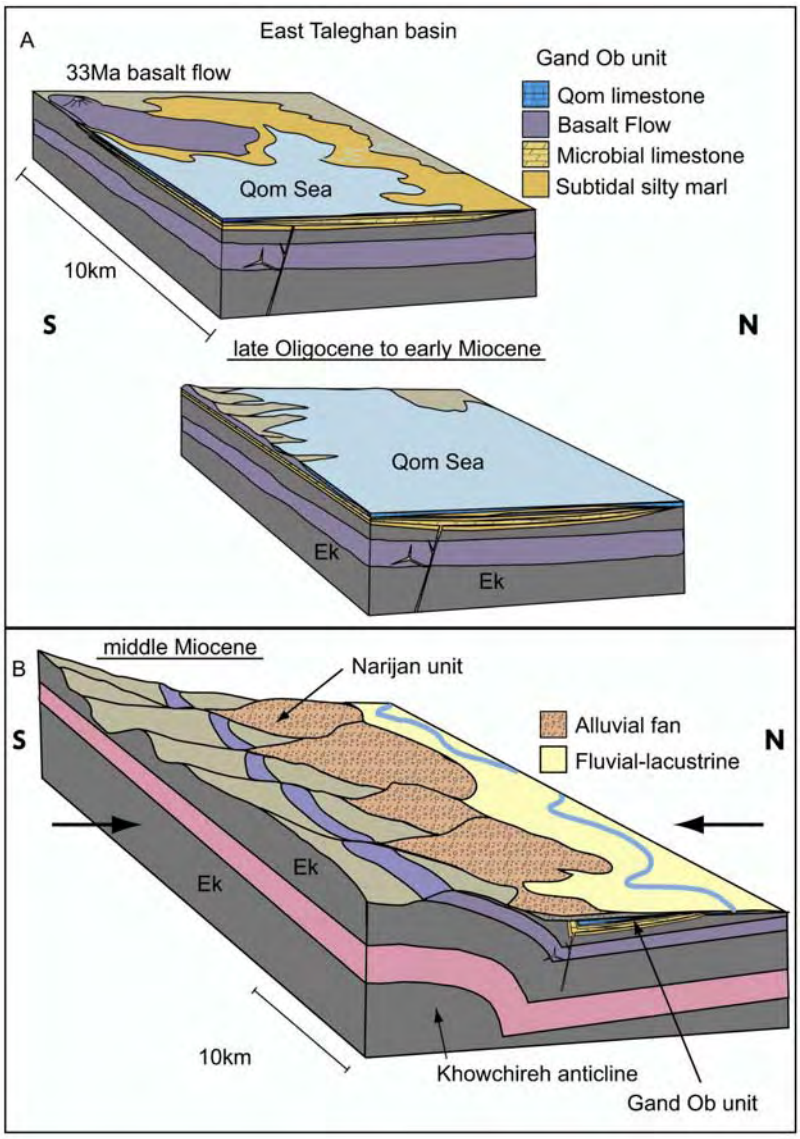

Figure 15. Schematic diagram for the Taleghan basin showing the Oligocene–early Miocene deposition of the Gand Ab unit and the middle Miocene onset of initial deposition of the Narijan unit. (a) The Gand Ab unit depositional system consisted of a shallow-marine lagoonal environment adjacent to volcanic highlands. The region experienced episodic marine incursions and deposition of carbonate facies bearing Rupelian to Burdigalian marine fossils. Nonmarine rocks include basalts, sheet sandstones, and rare pebble layers. (b) The onset of contraction coincided with a final marine regression and deposition of growth strata along the S margin of the Taleghan basin. The basin axis was dominated by fluvial and lacustrine facies.

and the basin became dominated by fluvial-lacustrine deposition that overlapped the older Narijan conglomeratic growth strata (Figure 16b). This depositional shift could be the product of retrogradation driven by increased tectonic subsidence [e.g., *Heller et al.*, 1988] or the effects of a wetter climate [*Blair*, 1986], although abundant evaporites and limited plant remains in the lacustrine facies suggest an arid climate. However, given the existence of structures on nearly all basin margins, we prefer to attribute the depositional shift to closure of drainage outlets by shortening-related uplift and ponding of sediment in an internally drained basin [e.g., *Horton et al.*, 2002; *Sobel et al.*, 2003].

[64] The timing of the shift from alluvial fan to fluvial-lacustrine deposition in the uppermost Narijan unit remains poorly constrained. Possible correlation of gravels unconformably capping the Narijan unit with the Quaternary Kahrizak Formation along the S foot of the Alborz [*Rieben*, 1955] suggests that the uppermost Narijan unit may corre-

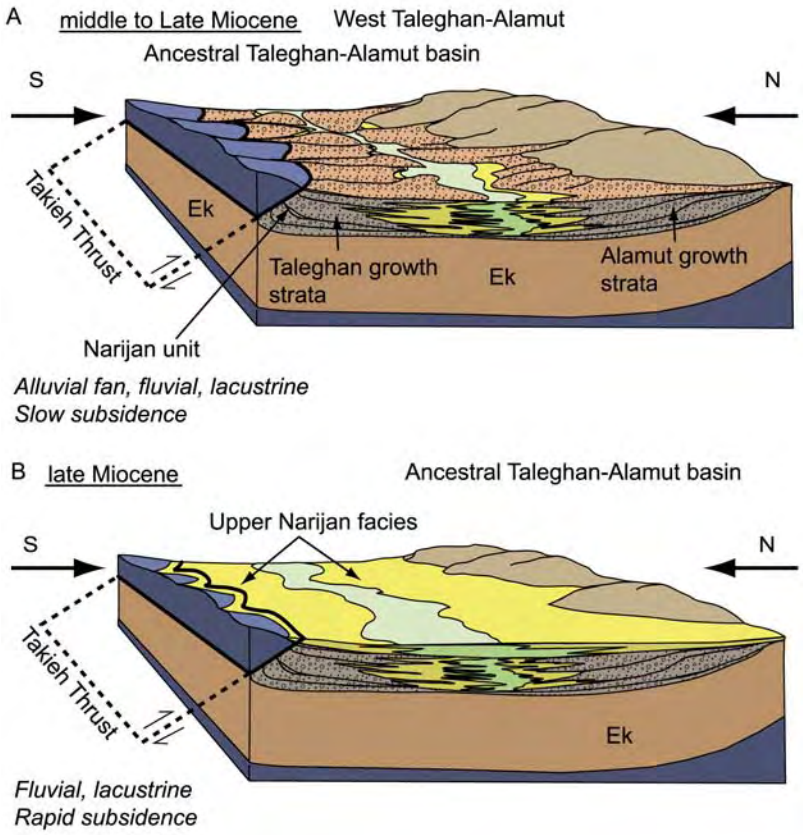

Figure 16. Schematic diagram for the ancestral Taleghan-Alamut basin showing the middle-late Miocene deposition of the Narijan unit. (a) The lower and middle Narijan unit includes alluvial fan facies containing growth strata along the S and N margins of the basin. These facies pass laterally toward the basin axis into finer grained fluvial and lacustrine facies. (b) The uppermost Narijan unit represents expansion of the lacustrine and fluvial facies belts, overlapping the alluvial fan facies of the lower and middle Narijan unit. This transition is attributed to closure of drainage outlets and ponding of sediment in an internally drained basin.

spond to the Hezardareh Formation directly beneath the Kahrizah strata [*Annells et al.*, 1975b]. The Hezardareh Formation is considered to be of late Miocene to Pliocene age on the basis of regional correlations and vertebrate fossils [*Stahl*, 1897; *Rieben*, 1955]. If these age inferences are correct, then the environmental shift observed in the uppermost Narijan unit probably occurred during late Miocene time and the end of Narijan deposition occurred in latest Miocene or conceivably earliest Pliocene time.

8. Evolution of the Western Alborz

8.1. Eocene-Oligocene Deformation

[65] One can explain deposition of the Oligocene–lower Miocene marine and nonmarine clastic rocks of the Gand Ab unit by flexural subsidence due to compression [*Brunet et al.*, 2003; *Vincent et al.*, 2005], fault-induced or thermal subsidence driven by extension [*Hassanzadeh et al.*, 2004], or alternatively, global sea level rise. Sea level rise is ruled out by the fact that the Oligocene–lower Miocene stratigraphic record across the Middle East shows a continual decrease in global sea level due to the formation of continental ice sheets in the southern hemisphere [*Haq et al.*, 1988; *Wilson et al.*, 1998; *Haq and Al-Qahtani*, 2005]. We therefore prefer a tectonic mechanism for the Oligocene–early Miocene regional transgression that covered central Iran and the southern Alborz.

[66] Eocene–earliest Oligocene conditions in the Alborz and in central Iran involved neutral to extensional tectonics [*Berberian*, 1983; *Brunet et al.*, 2003]. Eocene back-arc extension north of the Neotethyan magmatic arc (Urumieh-Dokhtar belt) paralleling the Zagros-Bitlis suture (Figure 1) probably created accommodation space for the >4-km-thick Karaj Formation [*Berberian*, 1983]. Intra-arc to back-arc extension in a rollback setting has been argued by *Hassanzadeh et al.* [2002, 2004] to have caused fault-related subsidence and postrift thermal subsidence in central to northern Iran, allowing the late Oligocene–early Miocene interior seaway to flood the former NW margin of the Urumieh-Dokhtar arc (Figure 15a). It is not clear when extension-related subsidence terminated, but the marine to nonmarine transition (from Qom to Upper Red Formation)

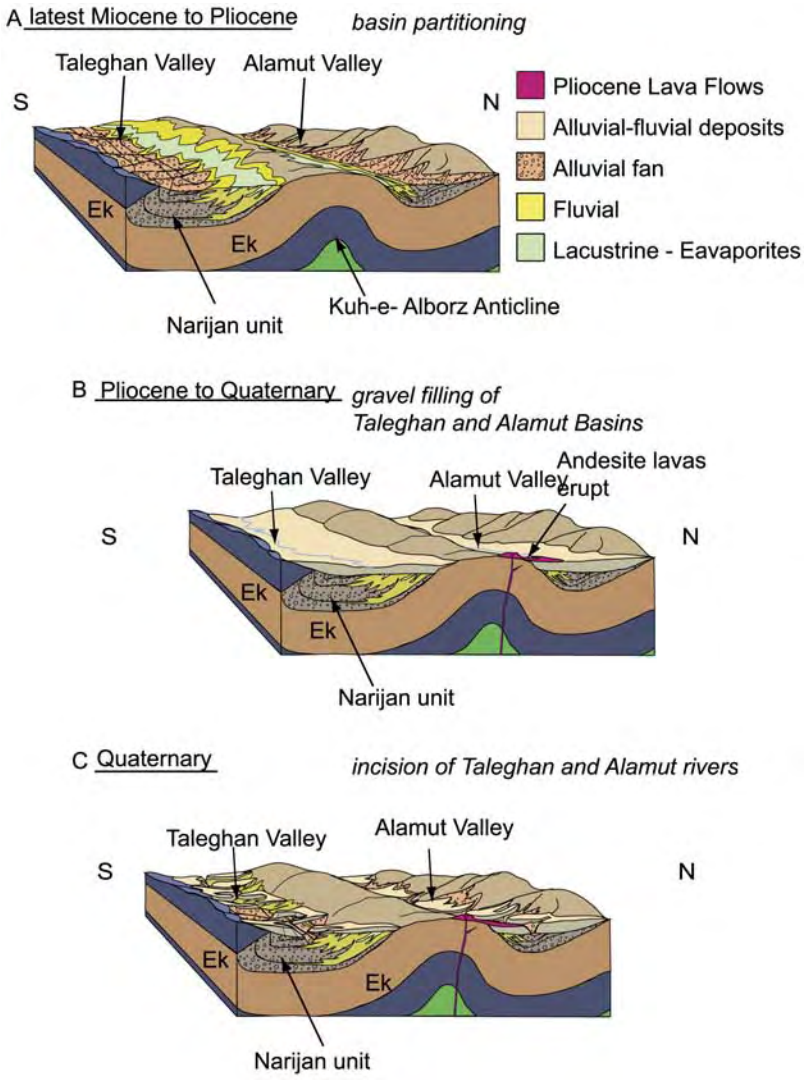

Figure 17. Schematic diagram showing the latest Miocene to Quaternary deformation and erosion of the Taleghan-Alamut basin system. (a) Continued contraction resulted in the growth of the Kuh-e-Alborz anticline that partitioned the ancestral Taleghan-Alamut basin and exposed the former basin axis to erosional recycling. (b) Rocks of the Narijan unit were exposed in Taleghan and Alamut basins, erosionally beveled, then overlain by Pliocene gravels. These were in turn overlain by Pleistocene lava flows. By this time, deformation had shifted to the S margin of the Alborz Mountains. (c) Uplift along the active S margin of the Alborz induced erosional down-cutting by the Taleghan and Alamut rivers, resulting in the present situation in which exposures of the deformed Taleghan and Alamut basins are partially covered by younger Pliocene–Quaternary deposits.

during the Burdigalian [*Stöcklin and Setudehnia*, 1977; *Amini*, 1991, 1997] suggests a fundamental shift in subsidence patterns at this time.

[67] Southward tilting of the Gand Ab unit prior to depositional overlap suggests that some tectonic activity affected E Taleghan basin before initial deposition of the Narijan unit (Figure 15b). It is not clear, however, whether tilting was related to the final phase of extension or to initial shortening recorded by Narijan growth strata. No angular discordance is observed between the Qom and Upper Red formations in central Iran [*Stöcklin and Setudehnia*, 1977], suggesting that tilting was limited to the Alborz region.

[68] Although we cannot conclusively rule out syndepositional shortening, sediment accumulation rates for the Gand Ab unit were less than 0.05 mm/yr, ~3–7 times lower than rates recorded in the Neogene foredeep of the Zagros fold-thrust belt [*Homke et al.*, 2004]. This discrepancy, and the northward onlap of younger levels of the Qom Formation [*Stöcklin and Setudehnia*, 1977; *Amini*, 1991,

1997], lead us to favor a model of postrift thermal subsidence for Oligocene–early Miocene accumulation in the Alborz.

8.2. Miocene Shortening

[69] Growth stratal relationships, paleocurrent data, clast count data, and correlation of the Narijan unit to the Upper Red Formation in central Iran provide evidence for a Miocene onset of shortening in the western Alborz Mountains. Deformational episodes began during middle Miocene time, including displacement on thrust structures along the S and N basin margins and attendant uplift of the Taleghan and northern Qazvin ranges to the S and a variety of individual ranges in the central Alborz to the N (Figure 15b). Timing is consistent with the ~12 Ma onset of rapid exhumation revealed by (U-Th)/He thermochronological data for the western Alborz [*Guest et al.*, 2006b].

[70] Clear evidence for middle Miocene contractional deformation comes from Narijan growth strata along the S edge of the Taleghan basin (Figure 16). The depositional age is poorly constrained, but the Narijan unit may be correlated with the middle to late Miocene Upper Red Formation south of the Alborz. Paleocurrents in the growth strata indicate a southern sediment source. The unroofing sequence in Narijan conglomerate suggests that Karaj lavas and underlying tuffs initially covered the source region and that exposure of Paleozoic and Mesozoic rocks occurred after deformation was underway. Similar Narijan conglomerates interpreted as possible growth strata along the N margin of Alamut basin are only moderately tilted (<40°), in contrast to the commonly overturned growth strata exposed along the S edge of Taleghan basin (Figures 4 and 5). This difference may be related to proximity to the bounding thrust fault or a lesser degree of syndepositional deformation along the N margin of the ancestral Taleghan-Alamut basin. Alamut conglomerates contain Paleozoic and Mesozoic clasts indicating a sediment source area to the north [*Annells et al.*, 1975b], probably the Kandavan thrust sheet (Figure 2).

[71] In W Taleghan basin, reverse slip along the Takieh fault caused progressive tilting during Miocene deposition of Narijan conglomerate. Paleocurrents indicate a southern source region in the northern Qazvin range, consistent with hanging wall uplift during motion on the Takieh fault. The lack of an unroofing sequence containing Mesozoic and Paleozoic rocks indicates less exhumation in the W, consistent with exposure levels in the northern Qazvin range. That the Takieh fault cuts the entire Narijan unit, including the uppermost fluvial-lacustrine rocks, indicates that displacement continued into late Miocene time.

[72] Similar to the S basin margin, the Narijan unit occurs in the footwall of the Kandavan thrust along the N edge of the Alamut basin and as preserved fragments along the Parachan thrust system defining the E limit of the Alamut and Taleghan basins. These footwall exposures of alluvial fan, fluvial, and lacustrine rocks are considered a record of southward encroachment of fold-thrust structures during evolution of the ancestral Taleghan Alamut basin.

8.3. Latest Miocene-Quaternary Deformation

[73] On the basis of crosscutting relationships, we identify deformation that occurred after late Miocene deposition of the uppermost Narijan unit but before deposition of Pliocene-Quaternary gravels. We propose that growth of the Kuh-e-Alborz anticline and resulting uplift of the axis of the ancestral Taleghan-Alamut basin (Figure 3) partitioned the basin into two internally deforming remnant basins (the Taleghan and Alamut basins) during latest Miocene time (Figure 17). Pliocene gravels and overlying andesitic lavas exhibit low dips (<5°–10°) probably related to primary deposition on gently sloping surfaces. This suggests that internal deformation within the basin system had largely ceased by the end of the Pliocene and had shifted to the S margin of the Alborz where deformation continues today [e.g., *Ritz et al.*, 2006].

[74] In W Taleghan basin the main strand of the N directed Taleghan fault zone placed Devonian rocks over a N strand of the fault zone and adjacent rocks of the upper Narijan unit. This implies fault activity in latest Miocene and younger time. Offset drainages and shutter ridges along the trace of the N strand further suggest recent activity [*Guest*, 2004; *Guest et al.*, 2006a].

9. Discussion

9.1. Middle Cenozoic Marine Ingression in the Alborz

[75] Discovery in the western Alborz of the edge the late Oligocene–early Miocene interior seaway, the system responsible for marine carbonate deposition of the Qom Formation throughout central Iran, is significant for several reasons. First, it places a limit on the northern extent of the seaway and, by inference, the spatial distribution of tectonic subsidence during Oligocene to middle Miocene time. *Hassanzadeh et al.* [2004] suggest that Oligocene–early Miocene subsidence was due to a period of extension in northern Iran that rifted the Neotethyan magmatic arc into two linear segments: the Alborz and the present Urumieh-Dokhtar belt. If correct, this hypothesis implies that the present Taleghan basin occupied the N edge of the rift zone and helps to explain the presence of local alluvial fan conglomerates within the lowermost basin fill (Oligocene–lower Miocene Gand Ab unit). The lack of a thick section may also imply that the major extensional structures are located south of the Alborz.

[76] Identifying the N margin of the late Oligocene–early Miocene Qom depositional region also allows for more accurate paleogeographic reconstructions. The shallow nearshore marine facies identified in the Gand Ab unit and the observed rapid lateral facies change from marine strata to nonmarine clastic rocks demonstrate that the Qom depositional extent in the western Alborz could not have extended much farther north than these exposures. This constraint coupled with the apparent lack of substantial Eocene–Oligocene strata in the northern Alborz and south Caspian basin [*Stöcklin*, 1974; *Berberian*, 1983; *Brunet et al.*, 2003] suggests that the region presently occupied by the axis of the Alborz Mountains had sufficient topographic

expression to separate the Caspian basin to the north from the Qom depositional area of central Iran (Figure 1). Although it is tempting to correlate this positive topography with the onset of collisional deformation [*Allen et al.*, 2003], the stratigraphic continuity of the Gand Ab unit with the Qom Formation of central Iran and the low rates of sediment accumulation and progressive onlap toward the Alborz suggest instead that these Oligocene–early Miocene rocks likely record postrift thermal subsidence or the final stages of Paleogene extension.

9.2. Collision-Related Syncontractional Sedimentation in the Alborz

[77] The middle to late Miocene Narijan unit, the major unit filling the ancestral Taleghan-Alamut basin, consists of clastic deposits containing growth strata linked to major thrusts and folds. The development of this basin adjacent to major contractional structures (the Takieh fault and Taleghan fault zone to the S and W and the Kandavan thrust to the N) signifies a switch from a neutral, or more likely extensional, tectonic regime to a contractional regime. We follow *Annells et al.* [1975b] in correlating the Narijan unit with the middle to late Miocene Upper Red Formation of central Iran on the basis of their analogous stratigraphic position above the Qom Formation and similar lithostratigraphy.

[78] The timing implied by this correlation suggests that shortening in the western Alborz region began in middle Miocene time. The Gand Ab-Narijan unconformity in the lower basin fill implies a depositional hiatus in the Alborz. A similar unconformity does not exist between the correlative Qom and Upper Red formations in central Iran, suggesting that the onset of Narijan deposition in the Alborz postdates the transition to Upper Red deposition. This consideration allows for the possibility that the initial Narijan deposition and associated shortening started near the end of the middle Miocene. Such an age would be consistent with results from recent thermochronological studies in the western Alborz which place the onset of rapid cooling and exhumation in this region at ~12 Ma [*Axen et al.*, 2001; *Guest et al.*, 2006b]. Although some workers consider the Oligocene to represent the onset of contractional uplift in the Alborz [e.g., *Brunet et al.*, 2003; *Allen et al.*, 2003], we emphasize that the Oligocene–early Miocene sedimentary record indicates marine conditions and low topography, inconsistent with uplift of a major source area in the Alborz.

[79] The timing of the Arabia-Eurasia collision remains controversial, with most estimates ranging from Late Cretaceous to late Miocene time [*Dewey et al.*, 1973; *Berberian and King*, 1981; *Hempton*, 1987; *Yilmaz*, 1993; *Alavi*, 1994; *Robertson*, 2000; *Axen et al.*, 2001; *McQuarrie et al.*, 2003; *Allen et al.*, 2004; *Agard et al.*, 2005; *Vincent et al.*, 2005]. The stratigraphic, sedimentologic, and geochronological data presented here indicate that coarse-grained sedimentation and synchronous shortening in the Taleghan-Alamut basin system of the western Alborz had commenced by late middle Miocene time. This estimate is in excellent agreement with an ~12 Ma onset of rapid exhumation revealed by (U-Th)/He thermochronological data for the same region [*Guest et al.*, 2006b].

[80] There is sufficient evidence from other studies to suggest that the ~12 Ma signal in the Alborz of northern Iran could be attributed to the onset of the Arabia-Eurasia collision. Examples include initial late Miocene construction of the Turkish-Iranian plateau [*Dewey and Sengor*, 1979; *Sengor and Kidd*, 1979], plate-circuit reconstructions and paleo-oceanographic data indicating final closure of the Neotethys Ocean by 14–10 Ma [*Woodruff and Savin*, 1989; *McQuarrie et al.*, 2003], and dated upper Miocene growth strata in the Zagros foreland basin [*Homke et al.*, 2004]. However, several new lines of evidence suggest that collisional deformation was already underway by the early Miocene. These data included improved age control for clastic fill in the most proximal part of the Zagros foreland basin [*Fakhari et al.*, 2005, 2007] and a (U-Th)/He record of rapid cooling in central Iran at ~20 Ma [*Verdel et al.*, 2007]. Given these constraints, we favor a model in which shortening induced by the Arabia-Eurasia collision had started across southern and central Iran by early Miocene time. Simultaneous deformation over such a broad region during collision is consistent with results from the northern Tibetan plateau which show that parts of central Asia thousands of kilometers from the suture zone began to deform upon initial collision of India [*Yin and Harrison*, 2000; *Horton et al.*, 2002, 2004; *Dupont-Nivet et al.*, 2004].

[81] The available data suggest a possible time lag between initial collision and the main phase of shortening in the Alborz of northern Iran, broadly consistent with a northward advance of deformation. Nevertheless, clear evidence of continued late Miocene and younger deformation in central Iran, the Zagros fold-thrust belt, and Alborz [*Axen et al.*, 2001; *McQuarrie et al.*, 2003; *Homke et al.*, 2004] demonstrates that these regions were not thickened sufficiently to induce an orderly spatial shift in deformation away from these regions, as proposed by some models [e.g., *England and Houseman*, 1985, 1989; *Allen et al.*, 2004]. Further data from additional regions are needed to assess whether the middle to late Miocene phase of deformation was a regional signal affecting the entire collision zone or was limited to the Alborz Mountains.

10. Conclusions

[82] 1. Lithostratigraphic similarities and new age control provided by a marine fossil assemblage and $^{40}Ar/^{39}Ar$ ages of interbedded lava flows indicate that the Gand Ab unit exposed in the lower part of the Taleghan basin in the western Alborz Mountains correlates with the Qom Formation of central Iran. These correlative units were deposited principally in marine lagoonal to lacustrine environments and represent the N margin of the late Oligocene–early Miocene interior seaway in central Iran. The low rates of sediment accumulation and progressive onlap toward the Alborz suggest that deposition was controlled by postrifting thermal subsidence rather than shortening-induced flexure.

[83] 2. The ~40-km-wide by 150-km-long, ancestral Taleghan-Alamut basin developed coeval with initial short-

ening in the western Alborz during middle Miocene time. Growth strata within the Narijan unit are expressed along the S and N basin margins, attesting to syncontractional sedimentation. Nonmarine depositional environments for the Narijan unit included basin-margin alluvial fans surrounding an axial system of fluvial and lacustrine deposition. Although not well constrained, a middle to late Miocene age is favored for the Narijan unit on the basis of new $^{40}Ar/^{39}Ar$ ages for crosscutting late Miocene and younger dikes and flows as well as a lithostratigraphic correlation to the Upper Red Formation of central Iran.

[84] 3. Crosscutting structures and overlapping stratigraphic relationships indicate that sediment accumulation in the ancestral Taleghan-Alamut basin ceased with the onset of late Miocene and Pliocene internal deformation that disrupted the basin by faulting and folding. The surface and rock uplift that accompanied this episode of basin partitioning led to the development of the modern Alborz Mountains. After Miocene time, deformation within the interior of the western Alborz had largely ceased, and folds and faults were erosionally beveled and overlapped by undeformed Pliocene to Quaternary gravels and localized lavas. At this time active faulting shifted to the S range margin where fault scarps and folded Quaternary gravels are observed.

[85] 4. Evolution of the ancestral Alamut-Taleghan basin constrains the onset of Neogene contractional deformation in the western Alborz. The clearest signal of initial shortening is recorded by middle Miocene basin fill, consistent with the ~12 Ma onset of rapid exhumation in the western Alborz determined independently by thermochronological methods [*Guest et al.*, 2006b]. Syndepositional shortening, uplift, and exhumation postdated the Arabia-Eurasia collision by ~10 Ma or more. Nevertheless, the synchroneity of initial Alborz shortening with widespread deformation in other tectonic elements of the Arabia-Eurasia collision zone, including the Zagros Mountains, Anatolia, and the Turkish-Iranian plateau, argues against models invoking large spatial and temporal shifts in the locus of collisional deformation.

[86] **Acknowledgments.** This research was supported by the National Science Foundation (grant EAR-9902932 to G. J. Axen), University of California, Los Angeles (UCLA) Council on Research (G. J. Axen), the University of Tehran Research Council (grant 651/1/328 to J. Hassanzadeh), and a UCLA Department of Earth and Space Sciences Cross-Training Fellowship (B. Guest and G. Peltzer). The insightful reviews returned two anonymous reviewers and an anonymous editor led to significant improvements in the plates and in the text.

References

Agard, P., J. Omrani, L. Jolivet, and F. Mouthereau (2005), Convergence history across Zagros (Iran): Constraints from collisional and earlier deformation, *Int. J. Earth Sci.*, *94*, 401–419.

Alavi, M. (1994), Tectonics of the Zagros orogenic belt of Iran: New data and interpretations, *Tectonophysics*, *229*, 211–238.

Alavi, M. (1996), Tectonostratigraphic synthesis and structural style of the Alborz Mountain system in northern Iran, *J. Geodyn.*, *21*, 1–33.

Allen, M., M. R. Ghassemi, M. Shahrabi, and M. Qorashi (2003), Accommodation of late Cenozoic oblique shortening in the Alborz range, northern Iran, *J. Struct. Geol.*, *25*, 659–672.

Allen, M., J. A. Jackson, and R. Walker (2004), Late Cenozoic re-organization of the Arabia-Eurasia collision and the comparison of short-term and long-term deformation rates, *Tectonics*, *23*, TC2008, doi:10.1029/2003TC001530.

Amini, A. (1991), Depositional environment and microfacies analysis of the F-member, Qum Formation, central Iran, M.S. thesis, 145 pp., Univ. of Tehran, Tehran.

Amini, A. (1997), Provenance and depositional environment of Upper Red Formation, central zone, Iran, Ph.D. dissertation, 320 pp., Univ. of Manchester, Manchester, U.K.

Annells, R. N., R. S. Arthurton, R. A. Bazley, and R. G. Davies (1975a), Explanatory text of the Qazvin and Rasht quadrangles map, Geol. Surv. of Iran, Tehran.

Annells, R. N., R. S. Arthurton, R. A. Bazley, and R. G. Davies (1975b), Geological quadrangle map of Iran, Qazvin and Rasht sheet, scale 1:250,000, Geol. Surv. of Iran, Tehran.

Annells, R. S., R. S. Arthurton, R. A. B. Bazley, R. G. Davies, M. A. R. Hamedi, and F. Rahimzadeh (1977), Geological map of Iran, Shakran sheet 6162, scale 1:100,000, Geol. Surv. of Iran, Tehran.

Ashley, G. M. (1990), Classification of large-scale subaqueous bedforms: A new look at an old problem, *J. Sediment. Pet.*, *60*, 160–172.

Axen, G. J., P. J. Lam, M. Grove, D. F. Stockli, and J. Hassanzadeh (2001), Exhumation of the west-central Alborz Mountains, Iran, Caspian subsidence, and collision-related tectonics, *Geology*, *29*, 559–562.

Berberian, M. (1983), The southern Caspian: A compressional depression floored by a trapped, modified oceanic crust, *Can. J. Earth Sci.*, *20*, 163–183.

Berberian, M., and G. C. P. King (1981), Towards a paleogeography and tectonic evolution of Iran, *Can. J. Earth Sci.*, *18*, 210–265.

Blair, T. C. (1986), Tectonic and hydrologic controls on cyclic alluvial fan, fluvial, and lacustrine rift-basin sedimentation, Jurassic-Lowermost Cretaceous Todos Santos Formation, Chiapas Mexico, *J. Sediment. Pet.*, *57*, 845–862.

Brunet, M. F., M. V. Korotaev, A. V. Ershov, and A. M. Nikishin (2003), The South Caspian Basin: A review of its evolution from subsidence modeling, *Sediment. Geol.*, *156*, 119–148.

Cant, D. J. (1978), Development of a facies model for sandy braided river sedimentation: Comparison of the South Saskatchewan River and Battery Point Formation, in *Fluvial Sedimentology*, *Can. Soc. Pet. Geol. Mem.*, vol. 5, edited by A. D. Miall, pp. 627–639, Can. Soc. of Pet. Geol., Calgary, Alberta, Canada.

Davoudzadeh, M., B. Lammerer, and K. Weber-Diefenbach (1997), Paleogeography, stratigraphy, and tectonics of the Tertiary of Iran, *Neues Jahrb. Geol. Palaeontol. Abh.*, *205*, 33–67.

DeCelles, P. G., M. B. Gray, K. D. Ridgway, R. B. Cole, P. Srivastava, N. Pequera, and D. A. Pivnik (1991), Kinematic history of a foreland uplift from Paleocene synorogenic conglomerate, Beartooth Range, Wyoming and Montana, *Geol. Soc. Am. Bull.*, *103*, 1458–1475.

Dewey, J. F., and A. M. C. Sengor (1979), Aegean and surrounding regions: Complex multiplate and continuum tectonica in a convergent zone, *Geol. Soc. Am. Bull.*, *90*, 84–92.

Dewey, J. F., W. C. Pitman III, W. B. F. Ryan, and J. Bonnin (1973), Plate tectonics and evolution of the Alpine system, *Geol. Soc. Am. Bull.*, *84*, 3137–3180.

Dupont-Nivet, G., B. K. Horton, R. F. Butler, J. Wang, J. Zhou, and G. L. Waanders (2004), Paleogene clockwise tectonic rotation of the Xining-Lanzhou region, northeastern Tibetan plateau, *J. Geophys. Res.*, *109*, B04401, doi:10.1029/2003JB002620.

England, P., and G. A. Houseman (1985), Role of lithospheric strength heterogeneities in the tectonics of Tibet and neighbouring regions, *Nature*, *315*, 297–301.

England, P., and G. Houseman (1989), Extension during continental convergence, with application to the Tibetan plateau, *J. Geophys. Res.*, *94*, 17,561–17,579.

Fakhari, M., G. J. Axen, B. K. Horton, A. Amini, J. Hassanzadeh, M. Ghavidel-Syooki, and S. A. Hosseini (2005), Revised age of the proximal Bakhtiyari Formation and implications for the evolution of the High Zagros, *Geol. Soc. Am. Abstr. Programs*, *37*, 58.

Fakhari, M. D., G. J. Axen, B. K. Horton, J. Hassanzadeh, and A. Amini (2007), Revised age of proximal deposits in the Zagros foreland basin and implications for Cenozoic evolution of the High Zagros, *Tectonophysics*, in press.

Ford, M., E. A. Williams, A. Artoni, J. Verges, and S. Hardy (1997), Progressive evolution of a fault-related fold pair from growth strata geometries, San Lorenc de Morunys, SE Pyrenees, *J. Struct. Geol.*, *19*, 413–441.

Ghibaudo, G. (1992), Subaqueous sediment gravity flow deposits: Practical criteria for their field description and classification, *Sedimentology*, *39*, 423–454.

Guest, B. (2004), The thermal, sedimentological and structural evolution of the central Alborz Mountains of northern Iran: Implications for the Arabia-Eurasia continent-continent collision and collisional processes in general, Ph.D. dissertation, 292 pp., Univ. of Calif., Los Angeles.

Guest, B., G. J. Axen, P. S. Lam, and J. Hassanzadeh (2006a), Late Cenozoic shortening in the west-central Alborz Mountains, northern Iran, by combined conjugate strike-slip and thin-skinned

deformation, *Geosphere*, *2*, 35–52, doi:10.1130/GES00019.1.

Guest, B., D. F. Stockli, M. Grove, G. J. Axen, P. S. Lam, and J. Hassanzadeh (2006b), Thermal histories from the central Alborz Mountains, northern Iran: Implications for the spatial and temporal distribution of deformation in northern Iran, *Geol. Soc. Am. Bull.*, *118*, 1507–1521.

Hampton, B. A., and B. K. Horton (2007), Sheetflow fluvial processes in a rapidly subsiding basin, Altiplano plateau, Bolivia, *Sedimentology*, doi:10.1111/j.1365-3091.2007.00875.x, in press.

Haq, B. U., and A. M. Al-Qahtani (2005), Phanerozoic cycles of sea-level change on the Arabian platform, *Geoarabia*, *10*, 127–160.

Haq, B., J. Hardenbol, and P. R. Vail (1988), Mesozoic and Cenozoic chronostratigraphy and cycles of sea-level change, in *Sea-Level Changes: An Intergrated Approach*, edited by C. K. Wilgus et al., *Spec. Publ. SEPM. Soc. Sediment. Geol.*, *42*, 71–108.

Harms, J. C., D. B. Mackenzie, and R. G. Walker (1982), Structures and sequences in clastic rocks, *Short Course 9*, Soc. of Econ. Paleontol. and Miner., Tulsa, Okla.

Harzhauser, M., W. E. Piller, and F. F. Steininger (2002), Circum-Mediterranean Oligo-Miocene biogeographic evolution—The gastropods' point of view, *Palaeogeogr. Palaeoclimatol. Palaeoecol.*, *183*, 103–133.

Hassanzadeh, J., A. M. Ghazi, G. Axen, B. Guest, D. F. Stockli, and P. Tucker (2002), Oligocene mafic-alkaline magmatism in north and northwest of Iran: Evidence for the separation of the Alborz from the Urumieh-Dokhtar magmatic arc, *Geol. Soc. Am. Abstr. Programs*, *34*, 331.

Hassanzadeh, J., G. Axen, B. Guest, D. F. Stockli, and A. M. Ghazi (2004), The Alborz and NW Urumieh-Dokhtar magmatic belts, Iran: Rifted parts of a single ancestral arc, *Geol. Soc. Am. Abstr. Programs*, *36*, 434.

Heizler, M. T., F. V. Perry, B. M. Crowe, L. Peters, and R. Appelt (1999), The age of Lathrop Wells volcanic center: An Ar-40/Ar-39 dating investigation, *J. Geophys. Res.*, *104*, 767–804.

Heller, P. L., C. L. Angevine, N. S. Winslow, and C. Paola (1988), Two-phase stratigraphic model of foreland-basin sequences, *Geology*, *16*, 501–504.

Hempton, M. R. (1987), Constraints on Arabian plate motion and extensional history of the Red Sea, *Tectonics*, *6*, 687–705.

Homke, S., J. Verges, M. Garces, H. Emami, and R. Karpuz (2004), Magnetostratigraphy of Miocene-Pliocene Zagros foreland deposits in the front of the Push-e Kush Arc (Lurestan Province, Iran), *Earth Planet. Sci. Lett.*, *225*, 397–410.

Horton, B. K. (1998), Sediment accumulation on top of the Andean orogenic wedge: Oligocene to Miocene basins of the Eastern Cordillera, southern Bolivia, *Geol. Soc. Am. Bull.*, *110*, 1174–1192.

Horton, B. K., and J. G. Schmitt (1996), Sedimentology of a lacustrine fan-delta system, Miocene Horse Camp Formation, Nevada, USA, *Sedimentology*, *43*, 133–155.

Horton, B. K., A. Yin, M. S. Spurlin, J. Zhou, and J. Wang (2002), Paleocene-Eocene syncontractional sedimentation in narrow, lacustrine-dominated basins of east-central Tibet, *Geol. Soc. Am. Bull.*, *114*, 771–786.

Horton, B. K., G. Dupont-Nivet, J. Zhou, G. L. Waanders, R. F. Butler, and J. Wang (2004), Mesozoic-Cenozoic evolution of the Xining-Minhe and Dangchang basins, northeastern Tibetan plateau: Magnetostratigraphic and biostratigraphic results, *J. Geophys. Res.*, *109*, B04402, doi:10.1029/2003JB002913.

James, N. P. (1984), Shallowing upward sequences in carbonates, in *Facies Models*, edited by R. D. Walker, pp. 213–228, Geol. Assoc. of Can., Toronto, Ontario, Canada.

Kendall, A. C. (1984), Evaporites, in *Facies Models*, edited by R. D. Walker, pp. 259–296, Geol. Assoc. of Can., Toronto, Ont., Canada.

Lowe, D. R. (1982), Sediment gravity flows: II. Depositional models with special reference to the deposits of high-density turbidity currents, *J. Sediment. Pet.*, *52*, 279–297.

McQuarrie, N., J. M. Stock, C. Verdel, and B. P. Wernicke (2003), Cenozoic evolution of Neotethys and implications for the causes of plate motions, *Geophys. Res. Lett.*, *30*(20), 2036, doi:10.1029/2003GL017992.

Miall, A. D. (1996), *The Geology of Fluvial Deposits: Sedimentary Facies, Basin Analysis, and Petroleum Geology*, 582 pp., Springer, New York.

Mohrig, D., K. X. Whipple, M. Hondzo, C. Ellis, and G. Parker (1998), Hydroplaning of subaqueous debris flows, *Geol. Soc. Am. Bull.*, *110*, 387–394.

Riba, O. (1976), Syntectonic unconformities of the Alto Cardener, Spanish Pyrenees: A genetic interpretation, *Sediment. Geol.*, *15*, 213–233.

Rieben, H. (1955), The geology of the Tehran plain, *Am. J. Sci.*, *253*, 617–639.

Ritz, J.-F., H. Nazari, A. Ghassemi, R. Salamati, A. Shafei, S. Solaymani, and P. Vernant (2006), Active transtension inside central Alborz: A new insight into northern Iran–southern Caspian geodynamics, *Geology*, *34*, 477–480.

Robertson, A. H. F. (2000), Mesozoic-Tertiary tectonic-sedimentary evolution of a south Tethyan oceanic basin and its margins in southern Turkey, in *Tectonics and Magmatism in Turkey and the Surrounding Area*, edited by E. Bozkurt et al., *Geol. Soc. Spec. Publ.*, *173*, 97–138.

Schuster, F., and U. Wielandt (1999), Oligocene and Early Miocene coral faunas from Iran: Palaeoecology and palaeobiogeography, *Int. J. Earth Sci.*, *88*, 571–581.

Sengor, A. M. C. (1990), A new model for the late Paleozoic-Mesozoic tectonic evolution of Iran and implications for Oman, in *The Geology and Tectonics of the Oman Region*, edited by M. P. Searle and A. C. Ries, pp. 797–831, Geol. Soc., London.

Sengor, A. M. C., and W. S. F. Kidd (1979), The post-collisional tectonics of the Turkish-Iranian plateau and a comparison with Tibet, *Tectonophysics*, *55*, 361–376.

Shultz, A. W. (1984), Subaerial debris-flow deposition in the upper Paleozoic Cutler Formation, western Colorado, *J. Sediment. Pet.*, *54*, 759–772.

Sieber, N. (1970), Zur Geologie des Gebietes sudlich des Taleghan-Tales Zentral Elburz (Iran), Ph.D. thesis, 126 pp., Eidg. Tech. Hochsch., Zurich.

Smith, G. A. (1986), Coarse-grained nonmarine volcaniclastic sediment: Terminology and depositional process, *Geol. Soc. Am. Bull.*, *97*, 1–10.

Sobel, E. R., G. E. Hilley, and M. R. Strecker (2003), Formation of internally drained contractional basins by aridity-limited bedrock incision, *J. Geophys. Res.*, *108*(B7), 2344, doi:10.1029/2002JB001883.

Stahl, A. F. (1897), Zur Geologie von Persien, Geognostische Beschreibung von Nord- und Zentral-Persien, *Petermanns Mitt.*, *26*, 122 pp.

Stöcklin, J. (1968), Structural history and tectonics of Iran: A review, *Am. Assoc. Pet. Geol. Bull.*, *52*, 1229–1258.

Stöcklin, J. (1974), Northern Iran: Alborz Mountains, in *Mesozoic-Cenozoic Orogenic Belts: Data for Orogenic Studies*, edited by A. M. Spencer, *Geol. Soc. Spec. Publ.*, *4*, 213–234.

Stöcklin, J., and A. Setudehnia (1977), Stratigraphic lexicon of Iran, *Rep. 18*, 376 pp., Geol. Surv. of Iran, Tehran.

Suppe, J., G. T. Chou, and S. C. Hook (1992), Rates of folding and faulting determined from growth strata, in *Thrust Tectonics*, edited by K. R. McClay, pp. 105–122, Chapman and Hall, London.

Suppe, J., F. Sabat, J. A. Munoz, J. Poblet, E. Roca, and J. Verges (1997), Bed-by-bed growth by kink-band migration: Sant Lorenc de Morunys, eastern Pyrenees, *J. Struct. Geol.*, *19*, 443–461.

Tucker, M. E. (1978), Triassic lacustrine sediments from South Wales: Shore zone clastics, evaporites and carbonates, in *Modern and Ancient Lake Sediments*, edited by A. Matter and M. E. Tucker, *Spec. Publ. Int. Assoc. Sedimentol.*, *2*, 205–224.

Verdel, C., B. P. Wernicke, J. Ramezani, J. Hassanzadeh, P. R. Renne, and T. L. Spell (2007), Tertiary Cordilleran-style metamorphic core complexes in the Saghand region of central Iran, *Geol. Soc. Am. Bull.*, *119*, 961–977.

Vincent, S. J., M. B. Allen, A. D. Ismail-Zadeh, R. Flecker, K. A. Foland, and M. D. Simmons (2005), Insights from the Talysh of Azerbaijan into the Paleogene evolution of the south Caspian region, *Geol. Soc. Am. Bull.*, *117*, 1513–1533.

Weirich, F. H. (1989), The generation of turbidity currents by subaerial debris flows, California, *Geol. Soc. Am. Bull.*, *101*, 278–291.

Wilson, G. S., A. P. Roberts, K. L. Verosub, F. Florindo, and L. Sagnotti (1998), Magnetobiostratigraphic chronology of the Eocene-Oligocene transition in the CIROS-1 core, Victoria Land margin, Antarctica: Implications for Antarctic glacial history, *Geol. Soc. Am. Bull.*, *110*, 35–47.

Woodruff, F., and S. M. Savin (1989), Miocene deep-water oceanography, *Paleoceanography*, *4*, 87–140.

Yilmaz, Y. (1993), New evidence and model on the evolution of the southeast Anatolian orogen, *Geol. Soc. Am. Bull.*, *105*, 251–271.

Yin, A., and T. M. Harrison (2000), Geologic evolution of the Himalayan-Tibetan orogen, *Annu. Rev. Earth Planet. Sci.*, *28*, 211–280.

G. J. Axen, Department of Earth and Environmental Science, New Mexico Institute of Mining and Technology, Socorro, NM 87801, USA.

B. Guest, Geology Section, Department of Geological and Environmental Sciences, Ludwig-Maximilians-University, Munich D-80333, Germany. (b.guest@iaag.geo.uni-muenchen.de)

J. Hassanzadeh, Department of Geology, University of Tehran, Tehran, Iran.

B. K. Horton, Institute for Geophysics and Department of Geological Sciences, Jackson School of Geosciences, University of Texas, Austin, TX 78712-0254, USA.

W. C. McIntosh, New Mexico Geochronology Research Laboratory, New Mexico Institute of Mining and Technology, Socorro, NM 87801, USA.